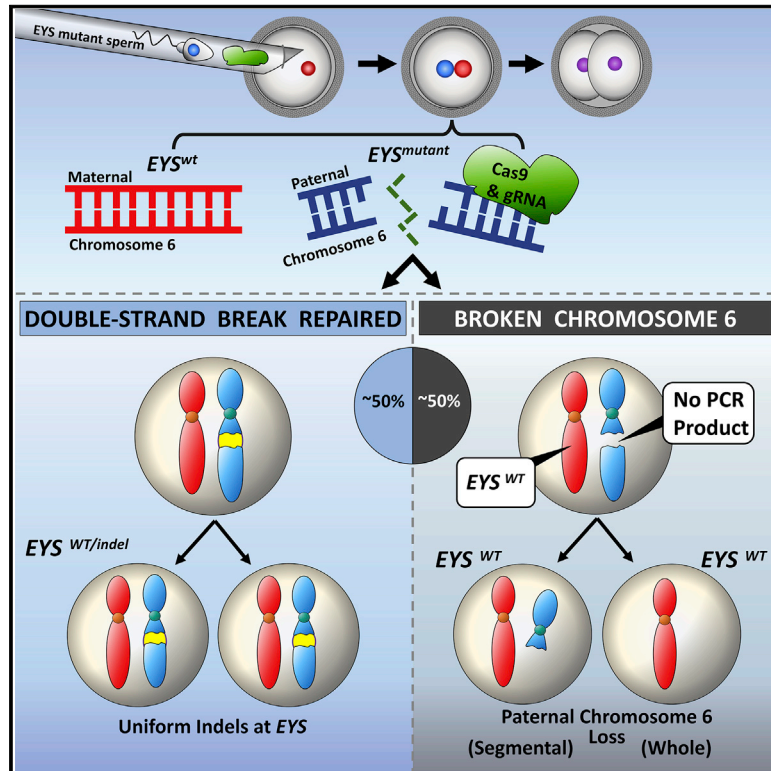


Allele-Specific Chromosome Removal after Cas9 Cleavage in Human Embryos

Graphical Abstract



Authors

Michael V. Zuccaro, Jia Xu, Carl Mitchell, ..., Rogerio Lobo, Nathan Treff, Dieter Egli

Correspondence

de2220@cumc.columbia.edu

In Brief

CRISPR-Cas9 gene editing in early human embryos leads to frequent loss of the targeted chromosome, indicating that human germline gene editing would pose a substantial risk for aneuploidy and other adverse genetic consequences

Highlights

- Cas9-mediated DSB induction and repair by end joining occurs within hours
- End joining provides an efficient way to restore reading frames without mosaicism
- Unrepaired DSBs persist through mitosis and result in frequent chromosome loss
- Off-target effects of Cas9 cause indels as well as chromosome loss

Article

Allele-Specific Chromosome Removal after Cas9 Cleavage in Human Embryos

Michael V. Zuccaro,^{1,2,8} Jia Xu,^{3,8} Carl Mitchell,² Diego Marin,³ Raymond Zimmerman,³ Bhavini Rana,^{3,4} Everett Weinstein,¹ Rebeca T. King,¹ Katherine L. Palmerola,⁵ Morgan E. Smith,¹ Stephen H. Tsang,^{2,6} Robin Goland,¹ Maria Jasin,⁷ Rogerio Lobo,⁵ Nathan Treff,^{3,4} and Dieter Egli^{1,2,5,9,*}

¹Department of Pediatrics and Naomi Berrie Diabetes Center, Columbia University, New York, NY 10032, USA

²Columbia University Stem Cell Initiative, New York, NY 10032, USA

³Genomic Prediction Inc., North Brunswick, NJ 08902, USA

⁴Department of Molecular Biosciences, Rutgers, The State University of New Jersey, New Brunswick, NJ 08854, USA

⁵Department of Obstetrics and Gynecology, Columbia University, New York, NY 10032, USA

⁶Departments of Ophthalmology, Pathology & Cell Biology, Columbia University, New York, NY, 10032, USA

⁷Developmental Biology Program, Memorial Sloan Kettering Cancer Center, New York, NY, 10065, USA

⁸These authors contributed equally

⁹Lead Contact

*Correspondence: de2220@cumc.columbia.edu

<https://doi.org/10.1016/j.cell.2020.10.025>

SUMMARY

Correction of disease-causing mutations in human embryos holds the potential to reduce the burden of inherited genetic disorders and improve fertility treatments for couples with disease-causing mutations in lieu of embryo selection. Here, we evaluate repair outcomes of a Cas9-induced double-strand break (DSB) introduced on the paternal chromosome at the *EYS* locus, which carries a frameshift mutation causing blindness. We show that the most common repair outcome is microhomology-mediated end joining, which occurs during the first cell cycle in the zygote, leading to embryos with non-mosaic restoration of the reading frame. Notably, about half of the breaks remain unrepaired, resulting in an undetectable paternal allele and, after mitosis, loss of one or both chromosomal arms. Correspondingly, Cas9 off-target cleavage results in chromosomal losses and hemizygous indels because of cleavage of both alleles. These results demonstrate the ability to manipulate chromosome content and reveal significant challenges for mutation correction in human embryos.

INTRODUCTION

Double-strand breaks (DSBs) stimulate recombination between homologous DNA segments (Jasin and Rothstein, 2013). The targeted introduction of a DSB followed by recombination allows for the precise modification of genomes in model organisms and cell lines and might be useful for the correction of disease-causing mutations in the human germline (NAS, 2017). DSBs occur during meiosis and are repaired through recombination between homologous chromosomes, thereby ensuring genome transmission and genetic diversity in offspring. Recombination between homologs is thought to be uncommon in mitotic cells, but was recently suggested to be efficient in fertilized eggs: a DSB at the site of a disease-causing mutation on the paternal chromosome resulted in the loss of the mutation such that approximately half of the resulting pre-implantation embryos carried only the maternal wild-type allele (Ma et al., 2017). The elimination was presumed to occur through use of the maternal genome as a repair template, resulting in what appeared as efficient correction of a pathogenic mutation on the paternal chromosome without mosaicism. This contrasts with frequent mosaicism

in previous studies with different cells of the same embryo carrying various edited and non-edited alleles (Liang et al., 2015).

The correction of pathogenic mutations through interhomolog recombination with a lack of mosaicism, if confirmed, would have major advantages over other approaches, given that it does not require the introduction of exogenous nucleic acids and is limited to alleles already present in the human population. However, alternative interpretations of the results have been proposed, including the loss of the paternal allele through deletions, chromosome loss, or translocations (Egli et al., 2018; Adikusuma et al., 2018). Thus, many questions remain regarding the outcomes of a DSB in human embryos, which we sought to address.

RESULTS

Allele-Specific Editing of the *EYS* Gene in Embryonic Stem Cells

To analyze outcomes of a Cas9 induced DSB, we recruited a patient with blindness as a sperm donor, carrying a homozygous G deletion mutation (rs758109813) in the gene encoding *EYS* associated with retinitis pigmentosa (Abd El-Aziz et al., 2008)

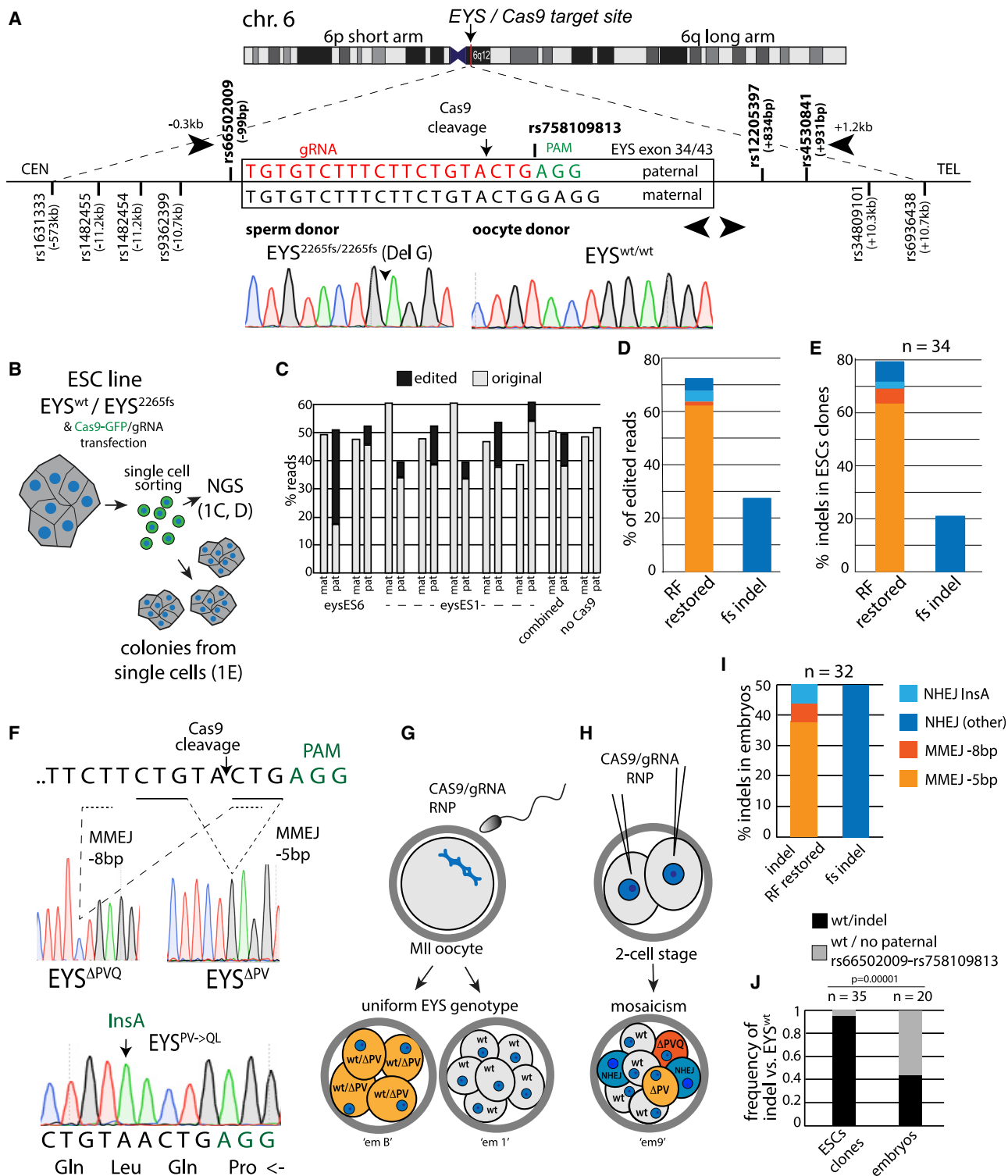


Figure 1. Efficient End Joining Within the First Cell Cycle after Cas9 RNP Injection at Fertilization.

(A) Schematic of genotypes at the human *EYS* locus with the paternal homozygous *EYS*^{2265fs} mutation. Alignment of paternal and maternal alleles, gRNA target, and flanking SNPs. Flanking primers (top arrowheads) were used for amplification and sequencing of the mutation site and linked SNPs within a single PCR product. Internal primers (bottom arrowheads) were used for Sanger sequencing and on-target NGS. Positions of SNPs and primers are indicated in relation to rs758109813. Abbreviations are as follows: CEN, centromere; TEL, telomere. Sanger sequences of genomic DNA of oocyte and sperm donor at the mutation site.

(legend continued on next page)

(Figure 1A). The *EYS* gene is located on chromosome 6, at 6q12 on the long arm, 3.5Mb from the centromere and the mutation results in the frameshift p.Pro2265Glnfs*46 (referred to as *EYS*^{2265fs}) in exon 34. A guide RNA (gRNA) was designed to target the mutant but not the wild-type allele, which differs at the protospacer adjacent motif (PAM) sequence. Pairing of the gRNA with the maternal allele at the 5'-AGG PAM site would require a 1 bp bulge, for which there is low tolerance (Lin et al., 2014). The Cas9 cleavage site occurs proximal to *EYS*^{2265fs}, such that small indels will preserve the original G deletion SNP, which can distinguish modified alleles of paternal or maternal origin. Furthermore, the mutation is flanked by SNPs rs66502009 centromeric to the mutation, rs12205397 and rs4530841 telomeric to the mutation, which are amplified within a ~1.5 kb PCR product, as well as by SNPs at ~10 kb away. Thus, differing homozygous SNPs allow the evaluation of novel combinations of maternal and paternal alleles (Table S1).

To determine the specificity of the gRNA for the mutant allele, we derived two embryonic stem cell (ESC) lines (eysES1 and eysES6) (Figure 1B). We transfected heterozygous ESCs for both the mutation site (*wt/EYS*^{2265fs}) and rs66502009 with Cas9-GFP and gRNA expression vectors to target the *EYS*^{2265fs} allele, and green fluorescent protein (GFP)-positive cells were harvested by flow cytometry. Using PCR and on-target next-generation sequencing (NGS) of seven independent biological samples consisting of a population of sorted cells, we scored for SNPs rs66502009 and *EYS*^{2265fs} to distinguish edited alleles of maternal or paternal origin. Fifty-one percent (199,780 of 392,672) were unmodified reads of the maternal *EYS*^{wt} allele, whereas 49% were of paternal origin, of which 11% (range 5%–33%, n = 7) were edited to contain small indels on reads containing the *EYS*^{2265fs} and the rs66502009 paternal allele (Figure 1C; Table S2). No modified maternal reads with an *EYS*^{wt} genotype were observed. This shows the specificity of the gRNA for the paternal allele in ESCs, resulting in efficient modification at *EYS*^{2265fs} (Table S2).

End Joining Restores the *EYS* Reading Frame by Inducing Predictable Indels in ESCs

Analysis of the types of edits in NGS reads showed that the most frequent event (63.5% of edited reads) was the deletion of 5 bp on the paternal allele (Figure 1D), resulting in the restoration of the reading frame. Deletion of 8 bp (1%) and insertion of 1 bp (3.5%), both of which restore the reading frame, as well as reading frame restorations from other indels (4.5%) were also observed. Another 27.5% of reads carried indels without reading

frame restoration. We also plated single cells for colony formation representing biologically independent editing events. In 245 clones (116 from eysES6 and 129 from eysES1), we identified 35 edited clones, 10 from eysES6 and 25 from eysES1 at a combined 14.3% editing efficiency. Thirty-four clones had indels in the paternal allele, whereas one had no detectable paternal allele at either rs66502009 or *EYS*^{2265fs}. Of the 34 clones with indels, the reading frame was restored in 27 (79.4%), primarily through a recurrent 5 bp deletion (Figure 1E). The placement of the gRNA results in cleavage between 2 identical regions of either 3 bp or 2 bp, defining sites of micro-homology (Figure 1F). Microhomology-mediated end joining (MMEJ) is a repair pathway that uses one to a dozen base pairs of homology (Sfeir and Symington, 2015). MMEJ at the *EYS* locus, as defined by the presence of microhomology, results in the deletion of either 5 bp or 8 bp, thereby restoring the reading frame, and generating novel alleles with deletions of either two amino acids (p.P2265-V2266) (*EYS*^{ΔPV}) or three amino acids (p.Pro2265_Gln2267del) (*EYS*^{ΔPVQ}). The deletion *EYS*^{ΔPV} was the most common single repair product. No mitotic recombination between *EYS*^{2265fs} and rs66502009, which would be indicative of interhomolog repair, was observed in the 34 edited clones.

EYS Reading Frame Restoration in Embryos

To determine editing outcomes in human embryos, we transferred *EYS*^{2265fs} mutant sperm through intracytoplasmic sperm injection (ICSI) together with a ribonucleoprotein (RNP) complex of Cas9 nuclease and the gRNA targeting *EYS*^{2265fs} (Figure 1G). Alternatively, Cas9/RNP was injected after fertilization at the two-cell stage (Figure 1H). Embryos were biopsied for genotyping at the cleavage or the blastocyst stage, respectively. Injection at the MII stage resulted in embryos (n = 7) that appeared uniform, for either an indel (n = 3), or only the *EYS*^{wt} allele (n = 4), whereas injection at the two-cell stage invariably resulted in mosaic embryos (n = 13) with up to three genotypes (Table S1). Combining both data from MII and two-cell-stage injections, we found a total of 32 end-joining events on the paternal allele that were independent, because they occurred in different embryos, or differed molecularly within the same embryo (Figure 1I; Table S1). Of these, 14 were MMEJ events, 12 of which resulted in a 5 bp deletion and 2 in an 8 bp deletion (Figure 1F). Furthermore, of a total of 18 independent nonhomologous end joining (NHEJ) events, defined by the absence of microhomology, 2 restored the reading frame through a 1 bp insertion, resulting in *EYS*^{PV > QL} (p.Pro2265_Val2266insGlnLeu) (Figure 1F). Importantly, in one

(B) Schematic of gRNA specificity testing in heterozygous ESCs. Forty-eight h after Cas9-GFP nucleofection, cells are harvested and used for on-target NGS of the mutation site and rs66502009.

(C) Read quantification of edited and original alleles in seven independent experiments of two cell lines. Abbreviation are as follows: Pat, paternal allele; mat, maternal allele.

(D and E) Type and frequency of indels in ESCs evaluated by using either on-target NGS (D) or colonies grown from single cells and Sanger sequencing (E).

(F) Schematic of DSB repair after Cas9 cleavage. Cas9 cleaves between two regions of microhomology (underlined). Sanger profiles of alternate repair products restoring the reading frame in human embryos through MMEJ or NHEJ. Arrowhead indicates direction of *EYS* transcription.

(G) Schematic of editing outcomes when mutant sperm is injected into the cytoplasm together with Cas9 RNP at the metaphase II (MII) stage. Abbreviation is as follows: RNP, ribonucleoprotein.

(H) Schematic of the injection performed after fertilization at the two-cell stage.

(I) Quantification of indels of combined data from MII and two-cell injections.

(J) Frequency of ESC clones or embryos with heterozygous indels versus clones or embryos with loss of paternal alleles and an *EYS*^{wt} genotype. Statistical analysis was performed using Fisher's exact test.

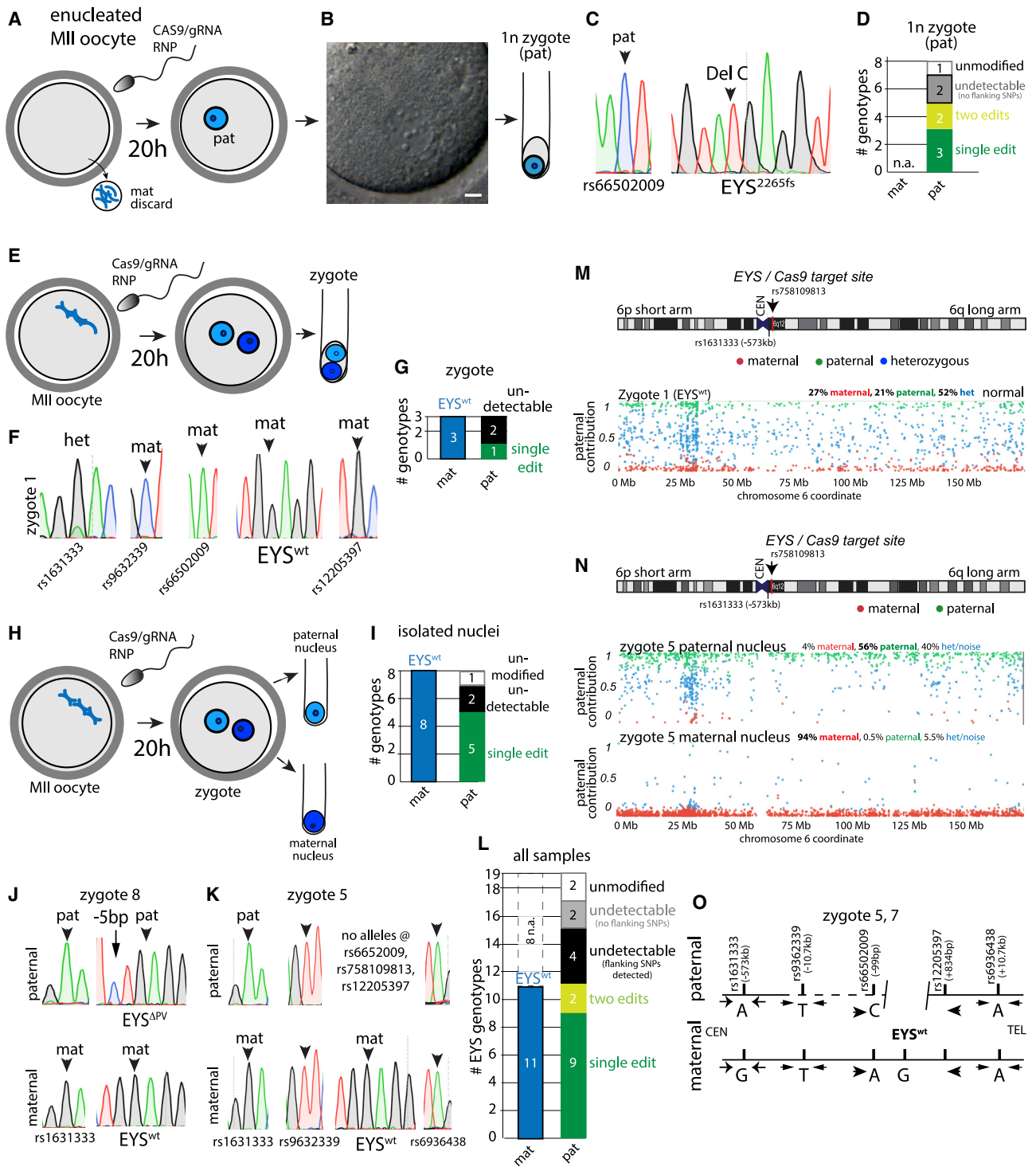


Figure 2. DSB Repair Occurs during the First Cell Cycle and Independent of the Maternal Genome

(A–D) Evaluating DNA repair outcomes in the absence of the maternal genome. A single sperm together with Cas9 RNP is injected into an enucleated oocyte (A), resulting in a 1PN zygote (B), followed by collection for genotyping (C). Scale bar, 10 μ m. Shown in (D) is the number of zygotes with each type of event. (E–G) Genotyping of whole two-pronuclear (2PN) zygotes at 20 h after Cas9 RNP injection and fertilization. Shown are (E) an experimental schematic, (F) Sanger sequence profiles, and (G) quantification of genotypes. (H–K) Genotyping of 2PN zygotes after isolation of paternal and maternal nuclei and separation to two different tubes for whole genome amplification. Shown are (H) an experimental schematic, (I) quantification of genotypes, (J) Sanger sequence profiles of a zygote with an indel, and (K) Sanger sequence profiles of a zygote with an undetectable paternal allele.

(legend continued on next page)

embryo derived from MII injection, all blastomeres (4 out of 4) showed uniform reading frame restoration through MMEJ, whereas the other 2 embryos had frameshift indels (Table S1).

Although DSB repair in ESCs and embryos both resulted in frequent indels, there was a significant difference in editing outcomes: considering both MII- and two-cell-stage injected embryos, 17 of 20 embryos contained cells with only an *EYS*^{wt} allele and the flanking maternal rs66502009 allele, representing at least 17 independent events; 12 embryos contained cells with indels and 9 embryos contained both types of cells. Therefore, the loss of the paternal allele was as or more common than a heterozygous indel in embryos (Figure 1J), whereas only a single event (2.8%) was seen in Cas9-treated ESC clones. These results indicate cell type differences in DSB repair and/or cell survival after a chromosome break.

Undetectable Paternal Alleles within the First Cell Cycle after Cas9 RNP Injection

EYS^{wt}-only detection could be due to unrepaired paternal alleles, undetectably modified paternal alleles (Adikusuma et al., 2018; Kosicki et al., 2018), or interhomolog repair, as previously suggested (Ma et al., 2017). Adikusuma and colleagues captured deletions of several hundred base pairs in 45% of mouse embryos by using a PCR assay spanning 1.6 kb flanking the Cas9 cut site. Similarly, the PCR assays spanning 1.5 kb used here (Figure 1A) would capture deletions of this type; however, the longest deletion found in 20 embryos on the paternal allele at the Cas9 cut site was 8 bp (Table S1). Although this does not rule out all deletions, deletions of a few hundred base pairs as found in mice do not account for the frequent *EYS*^{wt} genotypes.

To better understand the origin of *EYS*^{wt} genotypes, we analyzed events in the first cell cycle after MII injection of sperm and Cas9 RNP in either androgenetic zygotes with only a paternal genome, or zygotes with two pronuclei (2PN). These approaches also lead to a more conclusive determination of mosaicism, which is more reliably achieved when there is just a single cell and genome.

We first interrogated repair products in the absence of the maternal genome. The maternal genome was removed and discarded, and the *EYS*^{2265fs} mutant sperm was injected together with Cas9 RNP targeting the mutation site (Figure 2A). At 20 h after ICSI, embryos with a single paternal pronucleus were harvested for analysis (Figure 2B). Of eight androgenetic embryos from two different oocyte donors (five and three per donor), three contained a single small indel (Figure 2C), indicating end joining repair within the first cell cycle, whereas two contained two different modified alleles, indicative of repair after the onset of DNA replication but prior to mitosis. Of the remaining three,

one was unmodified and two failed to genotype at rs758109813 (Figure 2D; Table S1).

To determine whether the maternal genome can provide a repair template for the paternal genome, we performed ICSI with Cas9 RNP in nucleated oocytes (Figure 2E). We first controlled for accuracy of genotyping in zygotes with both alleles by amplifying single cells from embryos ($n = 3$) and single ESCs ($n = 4$) containing both genomes without exposure to Cas9. All cells showed heterozygosity at the mutation site and at rs66502009, demonstrating that both alleles were reliably detected (Table S1). We next analyzed 2PN zygotes 20 h after fertilization/Cas9 RNP injection. Of three zygotes, two showed only maternal alleles at the mutation site as well as at flanking SNPs within a ~22 kb window on either side (Figure 2F), whereas one showed an edited paternal allele (Figure 2G; Table S1). To account for the possibility of allele dropout in Sanger sequencing, on-target NGS showed no significant reads of either the paternal mutation or the flanking paternal SNP at rs66502009 (Table S2).

To directly determine whether recombination between paternal and maternal chromosomes could give rise to *EYS*^{wt/wt} embryos, we isolated individual paternal and maternal nuclei from zygotes at 20 h after ICSI and amplified them separately (Figure 2H). Genotyping at rs1631333 at 573 kb centromeric to the Cas9 cut site confirmed paternal or maternal origin (Figure S1). Of the eight paternal nuclei, five contained an indel on the paternal allele, whereas one was unmodified and two failed to genotype at the mutation site, but were successfully genotyped at flanking SNPs 10 kb away on both sides of the break (Figure 2I–2K; Table S1). All 5 genomes with indels showed only a single modification. Zygotes with an *EYS*^{wt} genotype in the maternal nucleus and no detectable *EYS* allele in the paternal nucleus would appear as *EYS*^{wt} when analyzed without physical separation of the two nuclei (as seen in Figure 2F). Because none of the zygotes contained a paternal genome with a wild-type *EYS* allele, there was no evidence for repair from the maternal genome among these eight zygotes.

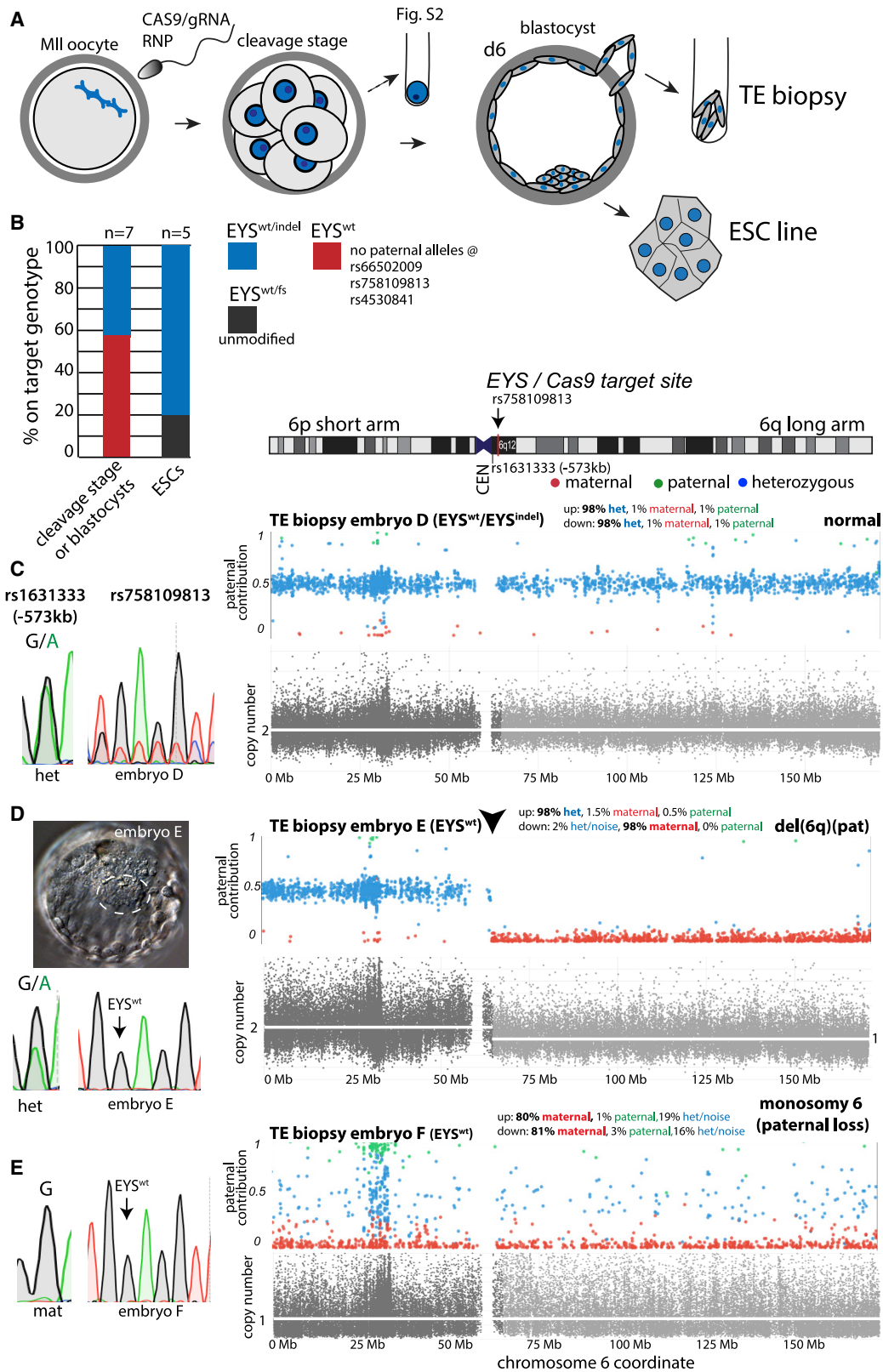
Considering all 19 zygotes (20 h after ICSI and Cas9 RNP), 11 of the paternal genomes were detectably modified by end joining during this first cell cycle, and two were unmodified (Figure 2L; Table S1). Editing predominantly gave rise to a single modification (9 out of 11 events) and thus non-mosaic zygotes, whereas 2 were mosaic. Although these mosaics were seen in androgenetic zygotes, they show that MII injection results predominantly, but not exclusively, in uniform editing.

The remaining 6 embryos had no detectable paternal allele at rs758109813. To determine the cause of paternal allelic loss, we also amplified and genotyped flanking SNPs. Neither of two

(L) Summary of all Sanger genotyping results of the paternal *EYS* locus at the one-cell stage at 20 h. The number of maternal and paternal nuclei is unequal because androgenesis excludes the maternal genome.

(M and N) Parent of origin analysis through SNP array. SNPs in which the maternal genotype was homozygous for one allele (red) and the paternal genotype was homozygous for the other allele (green) were used. Quantification of allelic frequencies is shown above the plots. up = chr6:1–64.7Mb, and down = chr6:64.7Mb–telomere. The increased signal around chr6:30Mb is in the HLA region, which shows increased background signal. Shown in (M) is the parent-of-origin analysis of a whole 2PN zygote (without polar body) with an *EYS*^{wt} genotype. Shown in (N) is the parent-of-origin analysis of separated nuclei isolated from 2PN zygotes through SNP array.

(O) Model for lack of a paternal allele: PCR amplification using flanking primers requires an intact DNA strand. In the presence of a maternal allele, the zygote appears as *EYS*^{wt}. Arrows and arrowheads indicate primer pairs. Abbreviations are as follows: CEN, centromere; TEL, telomere; pat, paternal; mat, maternal.



(legend on next page)

androgenotes showed amplification of flanking SNPs 10 kb distal and proximal to the Cas9 cleavage site and might therefore instead be because of amplification failure or extensive resection of the DSB. The two zygotes with only an *EYS*^{wt} genotype at rs758109813 as well as the two paternal nuclei extracted from 2PN zygotes but without an *EYS* on target genotype showed amplification at all flanking SNPs 10 kb away from the Cas9 cut site and were therefore successfully amplified (Table S1).

To more comprehensively analyze chromosome content, we performed genome-wide SNP array analysis. We first analyzed genomic DNA from sperm and oocyte donors to identify homozygous donor-specific alleles. Genomic DNA of an egg donor (Figure S1A) and genomic DNA of the semen donor (Figure S1B) showed homozygous alleles of maternal and paternal origin along chromosome 6. Only SNPs that were homozygous within the donors but different between donors were subsequently used for analysis.

We performed SNP array analysis of zygotes after Cas9 RNP injection at fertilization. Zygote 1 containing an *EYS*^{wt} genotype was successfully analyzed by using SNP arrays and signal from paternal and maternal alleles was seen all along chromosome 6 on both the p and q arms (Figure 2M). We also analyzed eight paternal and seven maternal nuclei isolated from eight 2PN zygotes (Figure 2N). Isolated individual nuclei uniformly showed either paternal or maternal origin, respectively, of chromosome 6 and other autosomes ($n = 326$ chromosomes) (Figures 2N and S1C). No exchange of chromosomes of paternal and maternal origin was observed (Tables S3 and S4). Therefore, paternal and maternal genomes remain physically separate during the first interphase, regardless of the presence of a DSB. The lack of a paternal genotype at *EYS* rs758109813 in two paternal nuclei and in zygote 1 was not due to loss of the paternal chromosome. Importantly, maternal alleles were detected in all (11 out of 11) zygotes, suggesting that the loss of the paternal allele is primarily biological, although technical causes cannot formally be excluded for two androgenetic zygotes without amplification of neighboring alleles.

Frequent Loss of Paternal *EYS*^{2265fs} in Pre-implantation Embryos but Not Derived ES Cell Lines

The loss of the paternal *EYS* allele from six zygotes might be because of an unrepaired DSB, which prevents amplification by PCR primers flanking the cut site (Figure 2O). Alternatively, a large insertion, deletion, or translocation would also prevent amplification of alleles rs66502009 to rs4530841 contained within the same PCR product. These different scenarios result in different outcomes in developing embryos. In the case of an

unrepaired break, chromosomal arms missegregate in mitosis. An insertion or deletion would be compatible with normal chromosome segregation patterns, whereas a translocation would affect two or more chromosomes.

To characterize the outcomes of a Cas9-induced DSB and the developmental potential of edited zygotes, we allowed them to develop to the cleavage or blastocyst stage for biopsy, genotyping, stem cell derivation, and karyotyping (Figure 3A). Of 18 oocytes injected with sperm and Cas9 RNP at the MII stage, 10 developed to the blastocyst stage (56%), which is within the normal frequency (Fogarty et al., 2017; Ma et al., 2017). At the cleavage stage, we biopsied individual blastomeres from 4 embryos, and at the blastocyst stage, we performed trophectoderm (TE) biopsies consisting of 5–10 cells from 3 embryos (Figure 3B). At the cleavage stage ($n = 4$ embryos), 2 embryos only had the maternal *EYS*^{wt} allele and flanking maternal SNPs, and 2 had indels on the paternal allele (Table S1). At the blastocyst stage ($n = 3$ embryos), 2 showed only the maternal *EYS*^{wt} allele (Table S1), which was confirmed by on-target NGS and allelic discrimination qPCR, and one showed an indel (Tables S2 and S5). Therefore, of 7 embryos, 4 (57%) had only a detectable *EYS*^{wt} allele (Figure 3B).

To generate ESCs with an *EYS*^{wt}-only genotype, 10 blastocyst-stage embryos were used for ESC derivation. Of these 10, 3 had been genotyped by Sanger sequencing, 2 of which were *EYS*^{wt} blastocysts. Five karyotypically normal ESC lines were obtained (Figure S2; Table S3), but despite the presence of a distinct inner cell mass and attachment to a feeder layer, ESC lines were not obtained from the two *EYS*^{wt} blastocysts, and cell death was observed within 3–4 days. Four cell lines showed an indel at the paternal mutation site, whereas one maintained an unmodified paternal allele (Figure 3B; Table S1). Thus, none of the ESC lines contained two wild type alleles, indicating no evidence for interhomolog repair. Combined with the 8 2PN zygotes tested for the presence of two wild type alleles (Figure S1; Table S1), none of the 13 samples showed interhomolog repair after MII injection.

The lack of evidence for interhomolog recombination suggests other explanations are likely for the presence of maternal only sequences at the mutation site. The loss of the paternal allele in embryos, together with a lack of their representation in ESC lines with only the *EYS*^{wt} allele, led us to investigate whether chromosomal changes accounted for the loss.

Segmental and Complete Loss of the Paternal Chromosome after Cas9 Cleavage in Embryos

To evaluate chromosome content in pre-implantation embryos, we first analyzed ESCs. ESC lines showed heterozygosity for

Figure 3. Chromosome Loss in Embryos with a “Wild-Type” Genotype

(A) Schematic of ICSI with Cas9 RNP at the MII stage followed by development to the cleavage and blastocyst stages. Analysis at the cleavage stage involves harvesting of all cells and is incompatible with further development, whereas trophectoderm biopsy at the blastocyst stage allows ESC derivation.

(B) On-target analysis by Sanger sequencing for embryos and embryonic stem cells.

(C–E) Heterozygosity analysis on chromosome 6 by SNP array, and Sanger sequencing profiles for the mutation site and for rs1631333, a SNP informative of parental origin located centromeric to the cut site. Parent-of-origin analysis through SNP array is shown. SNPs in which the maternal genotype was homozygous for one allele (red) and the paternal genotype was homozygous for the other allele (green) were used for analysis. Quantification of allelic frequencies is shown above the plots. Plot 2 (gray) indicates copy number, with flanking sides of rs758109813 shaded differently. up = chr6:1-64.7Mb, and down = chr6:64.7Mb-telomere. Shown in (C) is a blastocyst with a heterozygous indel. In (D) a blastocyst is shown with its *EYS*^{wt} Sanger genotype. Dotted line outlines the ICM.

(E) Analysis of a trophectoderm of another blastocyst.

parent-of-origin-specific SNPs along the entire chromosome 6 and throughout the genome because of the presence of maternal and paternal chromosomes (Figure S2; Table S3). We controlled for the effect of genome amplification used in embryo analysis by examining single, heterozygous human ESCs. Amplification of genomic DNA can alter the normal allelic ratio from 1:1 because of stochasticity. In both single amplified ESCs and trophectoderm biopsies of embryos that gave rise to the stem cell lines, heterozygous alleles were identified along the entire chromosome 6 and throughout the genome, albeit at a wider distribution than when a large number of cells are used (compare Figure S2B with Figure S2A with Figure S2C). For some SNPs, only one of the alleles reaches significance of detection and thus, in addition to heterozygous alleles (blue dots), paternal alleles (green dots) and maternal alleles (red dots) are detected (Figure S1C; Table S4). These controls provide a reference for the expected appearance of amplified genomic DNA in embryo samples.

We then examined trophectoderm biopsies from the three blastocyst embryos that had been genotyped at *EYS* by Sanger sequencing. Embryo D, which carried a heterozygous indel and gave rise to ESC line *eyes*ES9 (Table S1), showed heterozygosity and uniform signal intensity across chromosome 6 (Figure 3C). In contrast, one of the two *EYS*^{wt} blastocysts that had failed to develop a stem cell line (embryo E) showed loss of heterozygosity spanning the region from the Cas9 cut site at *EYS* to the telomere of paternal chromosome 6 (Figure 3D). The loss of heterozygosity at the *EYS* break site was paralleled by a loss of signal intensity because of copy number loss (Figure 3D). Therefore, loss of genetic material, rather than break-induced replication from the paternal centromere to the telomere is responsible for the absence of paternal SNPs. Furthermore, the other *EYS*^{wt} blastocyst (embryo F), which also failed to give rise to an ESC line, showed monosomy for the maternal chromosome 6, indicating loss of the entire paternal chromosome 6 (Figure 3E). Both blastocysts were euploid for other autosomes (Table S3).

To understand the process of chromosome loss, we performed analysis of chromosome content in blastomeres at the cleavage stage. We harvested 23 individual blastomeres from 4 embryos (Table S1). Two cleavage-stage embryos had a maternal-only genotype at *EYS*, which was confirmed by on-target NGS (Table S2). Four of six blastomeres with an *EYS*^{wt} Sanger genotype from one embryo (embryo 1) were analyzed by using SNP arrays and showed segmental rearrangement of paternal chromosome 6. Of the four cells, three had losses of chromosome 6q distal to the Cas9 cleavage site, as seen by SNP array, copy number analysis and by Sanger genotyping of parent-of-origin-specific SNPs (Figure S3A; Table S1). In one cell, chromosome 6q was gained, resulting in an overrepresentation of paternal SNPs distal to *EYS*, and an increase in copy number. In this cell, paternal SNPs were present at rs34809101 and rs6936438, 10 kb distal of the Cas9 cleavage site (Figure S3A, cell 4). Therefore, the loss of the paternal *EYS*^{2265fs} allele can occur both through segmental losses as well as through segmental gains. These segments might not be joined with the centromere-containing p arm, and therefore missegregate in mitosis and are not detectable with primers flanking the cut site (Figure S3A).

The other embryo (embryo C) had the *EYS*^{wt} allele at the mutation site in five blastomeres, two additional blastomeres had

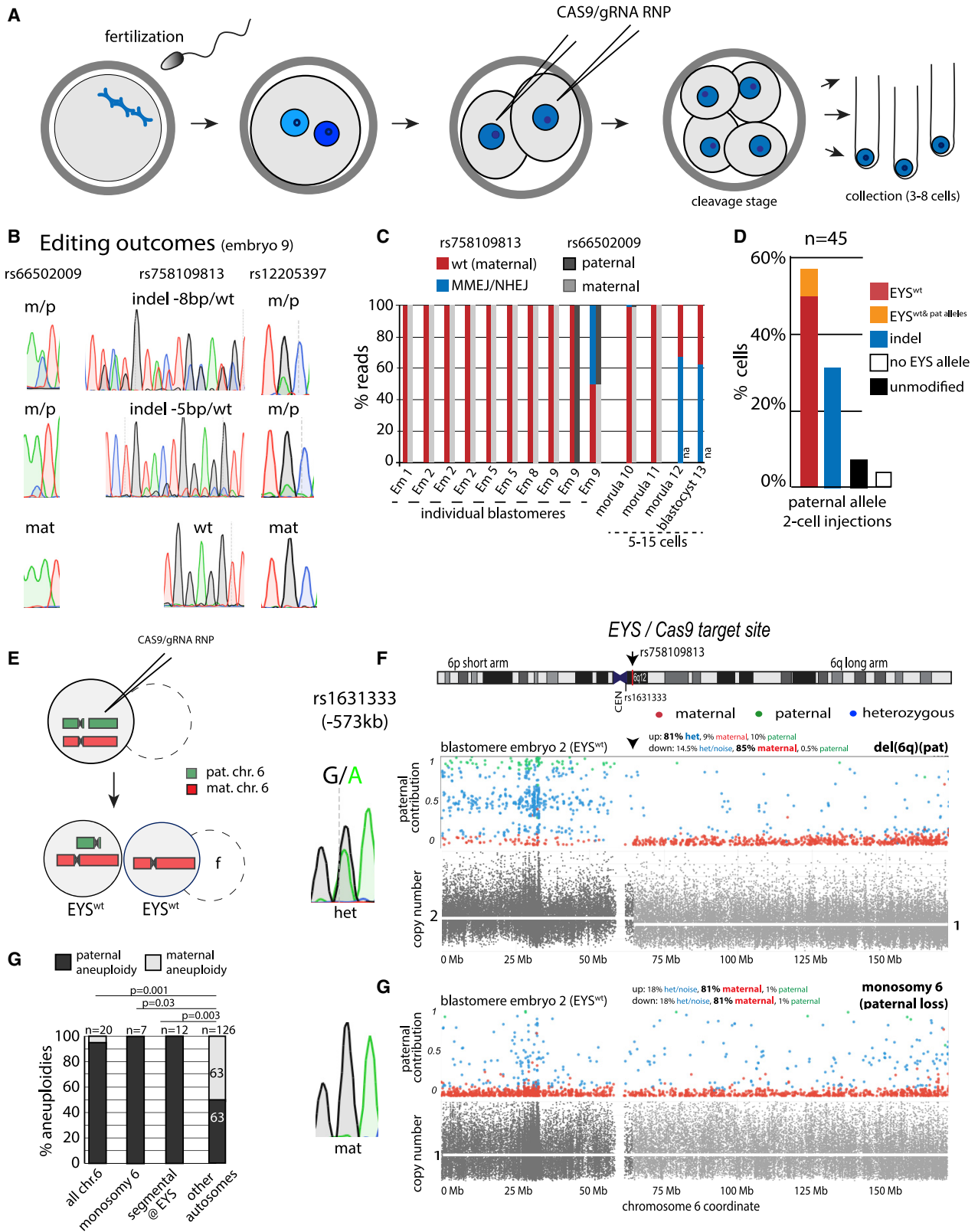
no on target genotype, and one had an indel on an *EYS*^{wt} (maternal) allele (Figure S3B; Table S1). Again, we found complementary losses and gains of paternal chromosome 6q. Four cells were monosomic for the maternal chromosome, one cell contained a gain of paternal chromosome 6q, and two cells contained only paternal chromosome 6p and were chaotic aneuploid. Therefore, Cas9 cleavage resulted in variable chromosome 6 content in cells with the same genotype *EYS*^{wt}. As in embryo 1, a paternal *EYS* allele was not detected in blastomeres containing only chromosome segments.

Blastomeres from the remaining two cleavage stage embryos showed repair by end joining of the paternal allele. One embryo (embryo B) showed a uniform deletion of 5 bp in all (4 out of 4) blastomeres. In the other embryo, 4 out of 5 blastomeres (embryo A) showed a net 2 bp indel and one cell showed a wild-type only genotype by Sanger sequencing, as well as by on-target NGS (Table S1). The one *EYS*^{wt} blastomere had monosomy 6 because of paternal loss. Blastomeres from the eight *EYS*^{wt/indel} cells showed heterozygosity and balanced copy number, except for one cell with a segmental deletion at chromosome 6q21 on the maternal chromosome, which is 40 Mb telomeric of the *EYS* locus (Figure S4). Three of the embryo A blastomeres had numerous aneuploidies on other autosomes (Table S3), which might be spontaneous and representative of the frequent mitotic abnormalities in human cleavage stage embryos (Vanneste et al., 2009; Ottolini et al., 2017).

In summary, of the 14 biopsies (12 blastomeres and 2 trophectoderm biopsies) with *EYS*^{wt} genotypes from 5 different embryos after Cas9 RNP injection at MII, all showed segmental or whole-chromosome aneuploidies of paternal chromosome 6 (Table S1). Thus, a common outcome of Cas9 RNP injections into MII oocytes is loss of paternal alleles because of segmental and whole-chromosome loss, which appear as *EYS*^{wt} cells in embryos characterized by on target sequencing (Table S1). Altogether, the loss of the paternal *EYS*^{2265fs} allele after Cas9 injection at fertilization occurs through aneuploidy, not efficient interhomolog repair.

Cas9 RNP Injection at the Two-Cell Stage Results in Chromosome Loss after a Single Mitosis

An obstacle to repairing the paternal allele through recombination between homologous chromosomes at the zygote stage is that paternal and maternal genomes are in two separate nuclei. To determine whether the maternal genome could provide a template for DSB repair when present with the paternal genome in the same nucleus, we injected Cas9 RNP into both cells of 13 two-cell stage embryos heterozygous for the *EYS* mutation and flanking SNPs (Figure 4A). Single blastomeres were harvested and amplified from 9 cleavage stage embryos, and 4 embryos were analyzed at the morula and blastocyst stages on day 5 after fertilization by using biopsies of multiple cells (Figure 4A). Embryos dissociated to single blastomeres showed mosaicism for multiple alleles (Figure 4B). Of a total of 45 genotyped single cells and day 5 biopsies, 25 (55%) showed an *EYS*^{wt} genotype at the mutation site and 12 (32%) showed end-joining events on the paternal allele; in the remaining, 3 showed end-joining events on the maternal allele, 3 showed no change, and 2 had no allele call even as flanking SNPs were detected (Figure 4D; Table S1).



(legend on next page)

Of the 25 samples with an *EYS*^{wt} genotype, 22 were maternal only at SNPs contained within the same PCR product (rs66502009 and rs12205397), 13 of which were maternal only also at flanking SNPs 10 kb proximal and 10 kb distal of the Cas9 cleavage site, whereas the remaining 9 showed heterozygosity at one or both 10 kb flanking sites (Table S1). Because Sanger sequencing is susceptible to allele-dropout, we performed on-target NGS on *EYS*^{wt} blastomeres from five embryos and confirmed the *EYS*^{wt} genotype (Figure 4C; Table S1). Paternal reads were detected in one morula (morula 10), at reduced representation compared with that of the maternal *EYS*^{wt} allele because of mosaicism (Figure 4C).

Interestingly, of the 25 *EYS*^{wt} samples, 3 cells from 3 different embryos showed flanking paternal SNPs, but no maternal SNPs on either side of the same PCR product (Figures S5A and S5B). NGS only detected a paternal allele at rs66502009 and only the maternal *EYS*^{wt} allele at rs758109813 (Figure 4D; Table S1). By array analysis, SNPs of both maternal and paternal origin were detected throughout chromosome 6, demonstrating that this cell contained both paternal and maternal chromosome 6 (Figure S5C). The novel linkages of maternal and paternal SNPs, present at a frequency of ~7% (3 out of 45), represent possible interhomolog repair events, although they are not readily explained through a simple gene conversion.

In 3 cells, we observed heterozygous indels on an allele with a wild-type SNP rs758109813. One such edit had also been observed in the MII injections in embryo C. Therefore, Cas9 RNP cut the maternal allele with an efficiency of 4 out of 84 (~5%), whereas in the same samples, editing of the paternal allele was 78 out of 84 (93%). Thus, the presence of the suboptimal PAM site allowed some cleavage of the maternal allele in the embryo, though with much lower efficiency than on the paternal allele.

To determine whether *EYS*^{wt} blastomeres were caused by paternal chromosome loss, we tested blastomeres of two embryos after a single mitosis post-Cas9/RNP injection for heterozygosity by using SNP arrays (Figures 4E–4G and S6). In one embryo, two sister blastomeres with an *EYS*^{wt} genotype showed loss of chromosome 6q and its sister cell showed monosomy 6 because of loss of the paternal chromosome (Figures 4F and 4G).

In the other embryo analyzed after a single mitosis, we found complementary loss of either paternal chromosomal arm 6q or 6p plus the centromere with breakpoints at the *EYS* locus (Fig-

ures S6A–S6D). The long arm that was lost in one blastomere was gained in the other, as seen by an increased representation of paternal SNPs in one of the two sister blastomeres on chromosome 6q (Figure S6C) and reciprocal copy number gain and loss on the q or the p arm (Figures S6B and S6C). In addition, one cell contained only chromosome 6p, no signal from chromosome 6q, and no other genomic DNA, and therefore is a cytoplasmic fragment (Figure S6D; Table S3). The exclusion of chromosomal arms in cytoplasmic fragments might be one mechanism of their elimination from the embryo. The reciprocal losses and gains of chromosomal arms were also observed by Sanger sequencing of rs1631333, located 573 kb from the Cas9 cleavage site toward the centromere (Figures S6B–S6D; Table S1). Loss of heterozygosity across the centromere as in Figure S5B is inconsistent with copy-neutral mitotic recombination, providing further support that the loss of paternal alleles occurred through the loss of genetic material rather than interhomolog recombination. Thus, Cas9 RNP injection at the two-cell stage can result in the loss of the paternal chromosome through missegregation in mitosis.

Considering karyotypes of all cells and biopsies from embryos injected with Cas9 RNP at fertilization or at the 2-cell stage, 19 out of 20 with loss of *EYS*^{2265fs} showed paternal specific abnormalities on chromosome 6. The one exception was a blastomere after two-cell-stage injection that contained flanking paternal alleles and might be due to interhomolog repair (Figure S5). Prior to the first cell division, the loss of paternal genotype might be due to an unrepaired or misrepaired break in a nucleus with a normal karyotype (Figure 2O), resulting in aneuploidies after mitosis. Aneuploidies of chromosome 6 were significantly enriched on the paternal chromosome for both segmental errors as well as whole chromosome loss (Figure 4G). In contrast, aneuploidies acquired after fertilization on the other autosomes equally affected both paternal and maternal chromosomes (50% versus 50%) (Figure 4G, Table S3). Thus, Cas9-induced cleavage in human embryos results in allele-specific segmental and whole chromosome errors beyond what is observed in normal development.

Cas9 Off-Target Effects Include Indels and Chromosome Loss

Spontaneous aneuploidies are common in human cleavage-stage embryos (Vanneste et al., 2009; Kort et al., 2016; Ottolini et al., 2017). In our dataset, 4 of 11 embryos injected at the MII

Figure 4. Chromosome Loss and Mosaicism after Cas9 RNP Injection into Two-Cell-Stage Embryos

- (A) Experimental schematic. A human oocyte is fertilized with *EYS*^{2265fs} mutant sperm and injected with Cas9 RNP at the two-cell stage, 30–35 h after ICSI, followed by analysis of individual cells after cleavage.
- (B) Sanger sequencing profiles of three different blastomeres (of eight total) of the same embryo (embryo 9).
- (C) On-target NGS of embryo samples at the mutation site (rs758109813) and the linked SNP rs66502009. Abbreviation is as follows: NA, not applicable, for samples without identifying parental SNP rs66502009; Em, embryo.
- (D) Quantification of the percentage of cells with indicated genotypes. No *EYS* allele represents samples without rs758109813, but with genotypes of distant flanking SNPs. *EYS*^{wt&pat} alleles represent cells with a novel combination of *EYS*^{wt} and paternal flanking SNPs within the same PCR product.
- (E and F) Analysis of sister blastomeres of an embryo after a single cell division after RNP injection. Shown in (E) is a schematic of the cell division products. Two cells were successfully analyzed by SNP array; no result was obtained for the second injected cell that did not divide (dotted line). Both sister cells are *EYS*^{wt}. Shown in (F) are SNP arrays and Sanger sequencing of rs1631333 informative of parental origin. Only SNPs in which the maternal genotype was homozygous for one allele (red) and the paternal genotype was homozygous for the other allele (green) were used for analysis. Quantification of allelic frequencies is shown above the plots. up = chr6:1–64.7Mb, and down = chr6:64.7Mb–telomere. Plot 2 (gray) indicates copy number, with flanking sides of rs758109813 shaded differently. Abbreviations are as follows: CEN, centromere; Pat, paternal; Mat, maternal.
- (G) Quantification of aneuploidies according to parental origin. Statistical analysis was done by using Fisher's exact test.

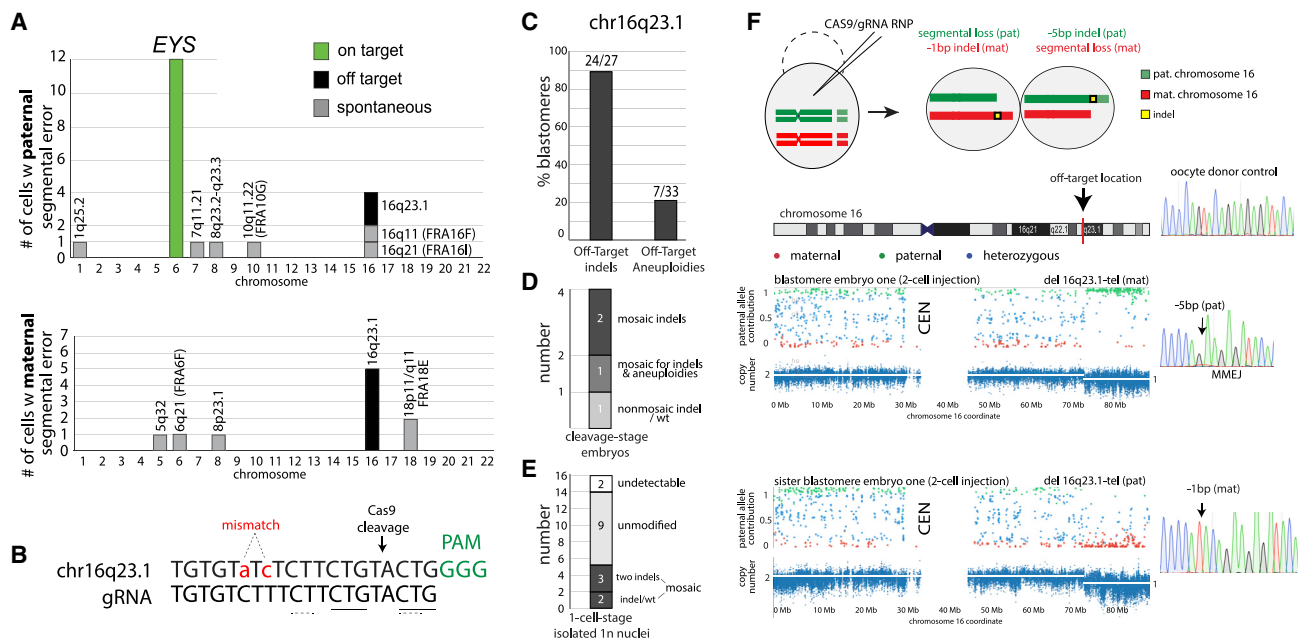


Figure 5. Aneuploidy and Indels Due to Cas9 Off-Target Activity on Chromosome 16

(A) Number of cells with segmental aneuploidies of maternal or paternal origin for each of chromosomes 1–22. Included are 38 blastomeres and blastocyst biopsies after MII or two-cell Cas9 RNP injections analyzed through SNP karyotyping (Table S3).

(B) Off-target site with two mismatches on chromosome 16q23.1. Underlined are regions of microhomology.

(C–F) Analysis of off-target activity on chromosome 16q23.1. Shown in (C) is the frequency of indels in 27 blastomeres, and of segmental aneuploidies in 33 blastomeres and blastocyst biopsies with chromosome 16 signal after MII or 2-cell Cas9 RNP injections. Shown in (D) is mosaicism in blastomeres after Cas9 RNP injection at fertilization. In (E) are genotypes in haploid (1n) nuclei at the one-cell stage at 20 h after fertilization and Cas9 RNP injection. In (F) is a SNP array analysis of sister blastomeres a single cell cycle after Cas9 RNP injection at the two-cell stage. Dotted circle indicates a cell of the same two-cell embryo without a result. SNPs in which the maternal genotype was homozygous for one allele (red) and the paternal genotype was homozygous for the other allele (green) were used. Blue indicates a heterozygous (normal) genotype. Plot 2 indicates copy number. Corresponding Sanger profiles at the off-target site are provided.

stage with Cas9 RNP contained aneuploidies on autosomes other than chromosome 6, which could be spontaneous or Cas9 induced if off-target sites are present. We focused on segmental errors to evaluate off-target aneuploidies, given that the genomic coordinates of chromosomal break points can be correlated with the location of predicted off-target sites.

Segmental errors of either paternal or maternal origin were found at 11 different sites (Figure 5A). All but two of the segmental errors were found only once, suggesting they occurred in a single cell during the second or third cell cycle after fertilization and Cas9 injection. Five mapped to common fragile sites. For instance, one site on the maternal chromosome 6q mapped to FRA6F telomeric of *EYS* and was found in one of five cells of an embryo injected with Cas9 RNP at fertilization (Figure S4A). However, segmental loss on chromosome 16q23.1 was recurrent in three of seven cleavage stage embryos (Figure 5A; Table S1).

To determine concordance with Cas9 off-target sites, we evaluated nine predicted off-target candidate sites for indels. One gRNA had two mismatches (Figure 5B), whereas others had three or more (Table S6). PCR and Sanger sequencing in four stem cell lines and three blastocysts revealed that only the site with two mismatches on chromosome 16q23.1 at location chr16:74344276 (hg37), showed indels in four of seven samples (Table S6). The site, which is present on both maternal and

paternal chromosomes, is concordant with the cytological location of recurrent segmental errors: chromosomal break sites in seven different cells mapped to chr16 between 74 Mb and 74.5 Mb at 16q22.3-23.1. No other predicted off-target sites were concordant with the location of singular segmental errors, which were therefore considered spontaneous (Figure 5A). The off-target site on chromosome 16 was then further examined for indels in a total of 27 cleavage stage blastomeres of 7 embryos. Off-target indels were identified in 24 blastomeres, one of which carried 2 different indels (Figure 5C; Table S1). In cleavage-stage embryos derived after MII injection of Cas9 RNP, three out of four embryos showed mosaic indels and just one was uniform (Figure 5D; Table S1).

To determine the timing of off-target activity, we analyzed isolated pronuclei containing either a maternal or a paternal genome at 20 h after fertilization and Cas9 RNP injection (Figures 2H and 5E). Of the 16 pronuclei, 5 showed heterozygous indels, 9 were unmodified, and 2 were undetectable (Figure 5E). Off-target indels included 5 bp and 8 bp deletions through MMEJ (Table S1). Interestingly (5 out of 5) modified nuclei were heterozygous at the 1-cell stage, carrying either an indel/wt allele (2 nuclei), or two different indels (3 nuclei), resulting from independent end-joining events on sister chromatids (Figure 5E). Thus, Cas9 cleavage at the off-target location occurred predominantly after the first S-phase, resulting in mosaicism.

Segmental chromosomal losses at chromosome 16q23.1 were found in 7 of 33 blastomeres and blastocyst biopsies (21%) with chromosome 16 signal (Figure 5C). One embryo, embryo one, derived after Cas9 RNP injection at the two-cell stage, carried different modifications on all four sister chromatids in both daughter cells (Figure 5F). One cell showed maternal segmental loss and an indel on the paternal allele, whereas the other carried paternal segmental loss and a different indel on the maternal allele. The parental origin of the chromosomes with the segmental error is identified through homozygous parent-of-origin-specific SNPs. Cells with an indel and a segmental loss on the other chromosome appeared homozygous by Sanger sequencing but are hemizygous (Figure 5F). Mosaic chromosome content and loss of heterozygosity of chromosome 16 was also seen in embryo C, obtained after MII injection of Cas9 RNP (Figure S7). All blastomeres carried a 6 bp insertion on one chromosome, which appeared heterozygous in some cells, and homozygous in others, depending on chromosomal content. Altogether, off-target activity of Cas9 results in both indels and segmental chromosomal changes.

DISCUSSION

The genome bestowed at fertilization determines much of our health as adults. Although genetic mutations might be corrected after birth by somatic gene therapy, the efficacy of this approach is dependent on the number of cells that can be edited, the ability to reverse damage that has already occurred, and disease-causing mutations will still be passed on to the next generation. In contrast, gene editing in the embryo will alter the genome of all cells, including the germline. An important requirement for clinical application is the ability to predict outcomes. Mosaicism prevents inferring the genotype of the fetus from a biopsy and is thus incompatible with clinical use. Therefore, the application of CRISPR/Cas9 prior to the first DNA replication in the embryo is meaningful (Ma et al., 2017). We injected CRISPR/Cas9 at fertilization with sperm, and found that in most, but not all instances, the outcome is non-mosaic editing. Temporally restricted activity of Cas9 to before DNA replication will likely be required to reliably avoid mosaicism.

Double-strand break repair in the embryo occurred predominantly through NHEJ or MMEJ. MMEJ restored the reading frame of the *EYS*^{2265fs} allele through the loss of two amino acids in relation to the wild-type allele, whereas NHEJ restored the reading frame through the insertion of a single A nucleotide, resulting in two amino acid substitutions. These recurrent 1 bp insertions are the consequence of filling in 1 bp overhangs created by Cas9 cutting (Lemos et al., 2018; Jasin, 2018). These novel *EYS* alleles, upon functional testing of the altered proteins, might be suitable for somatic gene therapy. In the germline, guidelines of the National Academies call for replacement of a disease-causing variant with a functional allele already common in the population (NAS, 2020).

We evaluated restoration of the wild-type sequence with the homologous chromosome as a template for DSB repair. After MII injection, no recombination between maternal and paternal genomes was seen. Although a lack of evidence with a limited number of samples does not rule out rare events, our data

show that interhomolog repair is not an efficient repair pathway at this stage of development. Novel combinations of maternal and paternal alleles representing possible interhomolog events were observed after two-cell-stage injections, although they were uncommon, and these embryos were mosaic.

Surprisingly, a frequent outcome of a single Cas9-induced DSB at the *EYS* locus is the loss of part or all of paternal chromosome 6. We found loss of the long arm 6q, the short arm 6p, as well as the entire chromosome. Embryos with an *EYS*^{wt} genotype showed aneuploidies of chromosome 6; by contrast, embryos with heterozygous edits *EYS*^{wt/indel} did not. Prior to mitosis, a zygote with an unrepaired or abnormally repaired DSB has no detectable paternal allele, and appears as *EYS*^{wt} in an on-target sequencing assay because of the presence of the intact maternal allele and euploid in an array or copy number analysis. In mitosis, unjoined chromosomal arms are converted to a segmental or whole-chromosome loss, which again appear as *EYS*^{wt} in on-target sequencing. Therefore, cells with the same *EYS*^{wt} genotype can have several different chromosome 6 contents. Different cells of the same embryo showed both whole-chromosome loss, as well as mirroring losses of the long or the short arms of chromosome 6. Therefore, pericentromeric cleavage at the *EYS* locus destabilizes the entire chromosome.

Chromosomal changes were also found at a Cas9 off-target cleavage site on chromosome 16. A difference between on-target and off-target activities were the degree of mosaicism after MII injection: on-target activity resulted in aneuploidies in all cells as well as uniform indels, whereas off-target activity resulted in mosaicism, both for aneuploidies and indels. This points to differences in the timing of cleavage in relation to replication at the one-cell stage, with the on-target site cleaved primarily before, and the off-target site primarily after replication.

Why a DSB is not reliably re-joined together to form an intact chromosome in the fertilized zygote is not currently known. It is possible that the DSB is repaired in ways that prevent rejoining, such as through addition of *de novo* telomeres. Addition of telomeres to a DSB can stabilize broken chromosomes including in mouse ESCs (Flint et al., 1994, Sprung et al., 1999). However, telomerase activity in human oocytes is low (Wright et al., 2001, Wright et al., 1996), and telomere extension occurs in a telomerase-independent manner in mouse cleavage divisions (Liu et al., 2007). Alternatively, the break might be left unrepaired for hours and persist through mitosis. The latter is consistent with the ability of human zygotes to enter mitosis with foci positive for γ H2AX, which marks DSBs (Chia et al., 2017). This suggests that checkpoint activation by one and perhaps multiple DSBs is insufficient to mediate cell cycle arrest and ensure repair at this stage of human development. This raises the intriguing possibility that endogenous DSBs contribute to mosaic aneuploidies and embryo loss. Although embryos with Cas9-induced aneuploidies cleave and can develop to the blastocyst stage, monosomic inner cell mass (ICM) cells did not establish stem cell lines. The loss of chromosome 6 might be compensated by maternal products provided in the egg, but is ultimately lethal. Indeed, pre-implantation embryos are tolerant of autosomal monosomies (Franasiak et al., 2014), but do not provide monosomic ESC lines (Biancotti et al., 2012).

Our results, summarized in Figure 6, serve as a cautionary note for the use of induced DSBs in editing the genome for

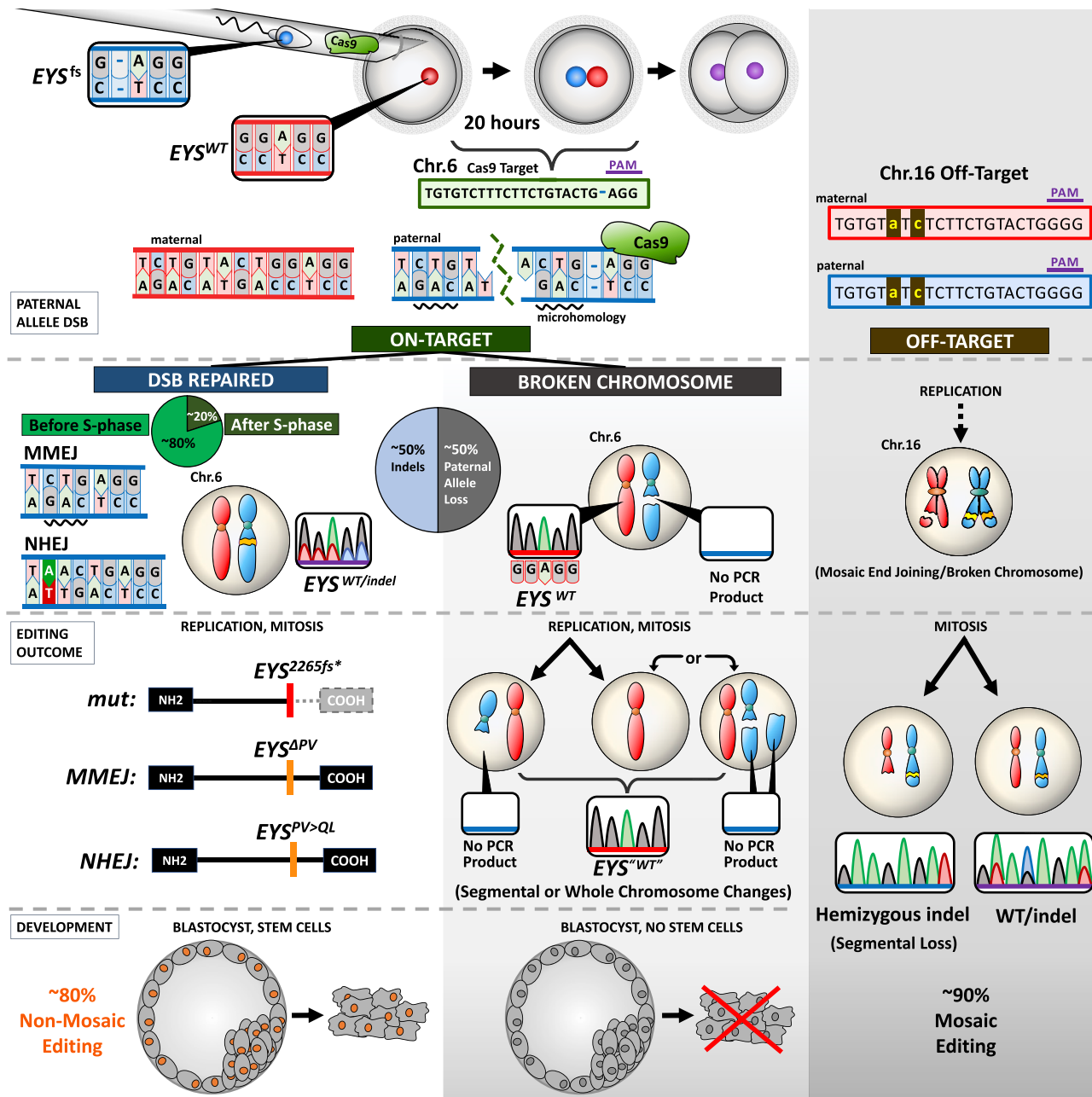


Figure 6. Visual Summary of Results

clinical use. Chromosomal material might be lost because of on-target and off-target activity of Cas9 and result in aneuploidy and developmental abnormalities. Upon further investigation, alternatives that do not require a DSB for mutation correction (Anzalone et al., 2019), such as base or prime editing, might be preferable to precisely correct mutations in the germline.

Our findings are likely relevant to the interpretation of a study using a guide RNA targeted to the MYBPC3 locus on chromosome 11 (Ma et al., 2017). Unrepaired breaks and the loss of the chromosomal arm or the entire chromosome might have

led to the loss of the mutant paternal allele, resulting in the detection of only a wild-type maternal allele by on-target sequencing. The karyotype of these embryos was not reported. Loss of paternal alleles distal, proximal, or on both sides of the Cas9 cleavage site (Ma et al., 2018) is reminiscent of segmental and whole chromosome 11 losses. Another study found segmental losses after Cas9 cleavage at POU5F1 (Alanis-Lobato et al., 2020). Whereas POU5F1 is located on the short arm of chromosome 6 at p21.3 ~27.5 Mb from the centromere, EYS is pericentromeric, with the cleavage site ~3.5 Mb from the centromere. The location of a DSB in relation to the centromere might have

different consequences for centromere function and induction of whole- or segmental-chromosome loss.

Our study suggests that a DSB induced by even a single gRNA can result in the allele-specific removal of a chromosome in human embryos. Previous studies in mouse embryos demonstrated elimination of sex chromosomes by targeting Cas9 to centromeric repeats or to multiple locations on the same chromosome (Zuo et al., 2017, Adikusuma et al., 2017). The finding that a single Cas9-induced cut can result in such outcome in human embryos suggests species-specific differences in repair or checkpoint control. Induction of allele-specific chromosome loss might have clinical applications. Aneuploidies caused by abnormal meiosis are common in human oocytes (Hassold and Hunt, 2001). Single chromosomal gains are estimated to occur in about 5% of human oocytes (McCoy et al., 2015), which might be amenable to correction by Cas9. Genotyping of oocyte donor and of both first and second polar bodies should allow inference of maternal-origin trisomy in fertilized zygotes. Because trisomies are from homologs or sister chromatids, which carry different SNPs because of recombination (Ottolini et al., 2015), most will have unique gRNA targets for Cas9-mediated removal in zygotes or two-cell embryos. Furthermore, carriers with Robertsonian translocation (t21;21) (Blouin et al., 1993) produce zygotes that are trisomic for chromosome 21, and thus removal of one chromosome might provide a path to a genetically related child without trisomy. However, prior to use in reproduction, we will need answers about the specific biology of the pre-implantation embryo: how DNA damage checkpoints respond to DSBs and the factors that determine end joining versus chromosome loss. Additional required knowledge includes how broken chromosomes are lost and whether fragmented chromosomes re-integrate in the genome. For any clinical application, challenges including, but not limited to avoiding off-target effects, remain. In a basic research context, Cas9 provides a powerful tool to understand DNA repair in the human pre-implantation embryo and the genetic and developmental consequences of DSBs.

STAR★METHODS

Detailed methods are provided in the online version of this paper and include the following:

- **KEY RESOURCES TABLE**
- **RESOURCE AVAILABILITY**
 - Lead Contact
 - Materials Availability
 - Data and Code Availability
- **EXPERIMENTAL MODEL AND SUBJECT DETAILS**
 - Gamete donation
 - Derivation and culture of ESCs
- **METHOD DETAILS**
 - RNP preparation
 - Oocyte manipulations
 - Genome amplification and Genotyping
 - EYS mutation allelic discrimination qPCR
 - Genome-wide SNP array
 - DSB repair in EYS^{wt}/EYS^{2265fs} ESCs
- **QUANTIFICATION AND STATISTICAL ANALYSIS**

SUPPLEMENTAL INFORMATION

Supplemental Information can be found online at <https://doi.org/10.1016/j.cell.2020.10.025>.

ACKNOWLEDGMENTS

We thank the New York Stem Cell Foundation and the Russell Berrie Foundation Program in Cellular Therapies for funding support; Briana Rudick for oocyte retrievals; Bob Prosser and the CUFC team for oocyte preparations; Chyuan-Sheng Lin for advice with Cas9 RNP injection; Michael Kissner for flow-cytometry training; Daniela Georgieva, Christine Lin, and Rudolph Leibel for critical reading; and Kathy Niakan for discussions. D.E. is a NYSCF - Robertson Investigator Alumnus.

AUTHOR CONTRIBUTIONS

M.V.Z. and D.E. designed the study. C.M., E.W., R.K., D.E., M.S., and M.V.Z. performed genotyping; D.E. micromanipulations; D.E. and M.V.Z. stem cell derivation; C.M., E.W., and M.V.Z. CRISPR experiments in ESCs; and B.R., R.Z., and D.M. performed SNP array and qPCR. K.L.P. contributed to one-cell experiments. N.T., D.M., and J.X. analyzed SNP array and qPCR data. R.L. recruited oocyte donors. S.H.T. provided expertise on EYS. M.J. contributed data interpretation but no experimental work or materials. R.S.G. provided study information. D.E. and M.V.Z. wrote the paper with contributions from all authors, particularly M.J.

DECLARATION OF INTERESTS

J.X., R.Z., B.R., D.M., and N.T. are employees or shareholders of Genomic Prediction. S.H.T. is a consultant for SPARK Therapeutics and has grants from Abenova Therapeutics. Dieter Egli is a member of the Cell Advisory Board.

Received: May 21, 2020

Revised: September 2, 2020

Accepted: October 14, 2020

Published: October 29, 2020

REFERENCES

- Abd El-Aziz, M.M., Barragan, I., O'Driscoll, C.A., Goodstadt, L., Prigmore, E., Borrego, S., Mena, M., Pieras, J.I., El-Ashry, M.F., Safieh, L.A., et al. (2008). EYS, encoding an ortholog of *Drosophila* spacemaker, is mutated in autosomal recessive retinitis pigmentosa. *Nat. Genet.* **40**, 1285–1287.
- Adikusuma, F., Williams, N., Grutzner, F., Hughes, J., and Thomas, P. (2017). Targeted Deletion of an Entire Chromosome Using CRISPR/Cas9. *Molecular therapy: the journal of the American Society of Gene Therapy*, **25**, 1736–1738.
- Adikusuma, F., Piltz, S., Corbett, M.A., Turvey, M., McColl, S.R., Helbig, K.J., Beard, M.R., Hughes, J., Pomerantz, R.T., and Thomas, P.Q. (2018). Large deletions induced by Cas9 cleavage. *Nature* **560**, E8–E9.
- Alanis-Lobato, G., Zohren, J., Mccarthy, A., Fogarty, N.M.E., Kubikova, N., Hardman, E., Greco, M., Wells, D., Turner, J.M.A., and Niakan, K.K. (2020). Frequent loss-of-heterozygosity in CRISPR-Cas9-edited early human embryos. *bioRxiv*. <https://doi.org/10.1101/2020.06.05.135913>.
- Anzalone, A.V., Randolph, P.B., Davis, J.R., Sousa, A.A., Koblan, L.W., Levy, J.M., Chen, P.J., Wilson, C., Newby, G.A., Raguram, A., and Liu, D.R. (2019). Search-and-replace genome editing without double-strand breaks or donor DNA. *Nature* **576**, 149–157.
- Biancotti, J.C., Narwani, K., Mandefro, B., Golan-Lev, T., Buehler, N., Hill, D., Svendsen, C.N., and Benvenisty, N. (2012). The in vitro survival of human monosomies and trisomies as embryonic stem cells. *Stem Cell Res. (Amst.)* **9**, 218–224.
- Blouin, J.L., Avramopoulos, D., Pangalos, C., and Antonarakis, S.E. (1993). Normal phenotype with paternal uniparental isodisomy for chromosome 21. *Am. J. Hum. Genet.* **53**, 1074–1078.

- Chen, A.E., Egli, D., Niakan, K., Deng, J., Akutsu, H., Yamaki, M., Cowan, C., Fitz-Gerald, C., Zhang, K., Melton, D.A., and Eggan, K. (2009). Optimal timing of inner cell mass isolation increases the efficiency of human embryonic stem cell derivation and allows generation of sibling cell lines. *Cell Stem Cell* 4, 103–106.
- Chia, G., Agudo, J., Treff, N., Sauer, M.V., Billing, D., Brown, B.D., Baer, R., and Egli, D. (2017). Genomic instability during reprogramming by nuclear transfer is DNA replication dependent. *Nat. Cell Biol.* 19, 282–291.
- Ding, Q., Regan, S.N., Xia, Y., Ostrom, L.A., Cowan, C.A., and Musunuru, K. (2013). Enhanced efficiency of human pluripotent stem cell genome editing through replacing TALENs with CRISPRs. *Cell Stem Cell* 12, 393–394.
- Egli, D., Zuccaro, M.V., Kosicki, M., Church, G.M., Bradley, A., and Jasin, M. (2018). Inter-homologue repair in fertilized human eggs? *Nature* 560, E5–E7.
- Flint, J., Craddock, C.F., Villegas, A., Bentley, D.P., Williams, H.J., Galanello, R., Cao, A., Wood, W.G., Ayyub, H., and Higgs, D.R. (1994). Healing of broken human chromosomes by the addition of telomeric repeats. *Am. J. Hum. Genet.* 55, 505–512.
- Fogarty, N.M.E., McCarthy, A., Snijders, K.E., Powell, B.E., Kubikova, N., Blakeley, P., Lea, R., Elder, K., Wamaitha, S.E., Kim, D., et al. (2017). Genome editing reveals a role for OCT4 in human embryogenesis. *Nature* 550, 67–73.
- Franasiak, J.M., Forman, E.J., Hong, K.H., Werner, M.D., Upham, K.M., Treff, N.R., and Scott, R.T. (2014). Aneuploidy across individual chromosomes at the embryonic level in trophoctoderm biopsies: changes with patient age and chromosome structure. *J. Assist. Reprod. Genet.* 31, 1501–1509.
- Hassold, T., and Hunt, P. (2001). To err (meiotically) is human: the genesis of human aneuploidy. *Nat. Rev. Genet.* 2, 280–291.
- Hastings, P.J., Ira, G., and Lupski, J.R. (2009). A microhomology-mediated break-induced replication model for the origin of human copy number variation. *PLoS Genet.* 5, e1000327.
- ISSCR (2016). Guidelines for Stem Cell Research and Clinical Translation, In: ISSCR.
- Jasin, M. (2018). Under the Influence: Cas9 Ends and DNA Repair Outcomes. *Crispr j.* 1, 132–134.
- Jasin, M., and Rothstein, R. (2013). Repair of strand breaks by homologous recombination. *Cold Spring Harb. Perspect. Biol.* 5, a012740.
- Kort, D.H., Chia, G., Treff, N.R., Tanaka, A.J., Xing, T., Vensand, L.B., Micucci, S., Prosser, R., Lobo, R.A., Sauer, M.V., and Egli, D. (2016). Human embryos commonly form abnormal nuclei during development: a mechanism of DNA damage, embryonic aneuploidy, and developmental arrest. *Hum. Reprod.* 31, 312–323.
- Kosicki, M., Tomberg, K., and Bradley, A. (2018). Repair of double-strand breaks induced by CRISPR-Cas9 leads to large deletions and complex rearrangements. *Nat. Biotechnol.* 36, 765–771.
- Lemos, B.R., Kaplan, A.C., Bae, J.E., Ferrazzoli, A.E., Kuo, J., Anand, R.P., Waterman, D.P., and Haber, J.E. (2018). CRISPR/Cas9 cleavages in budding yeast reveal templated insertions and strand-specific insertion/deletion profiles. *Proc. Natl. Acad. Sci. USA* 115, E2040–E2047.
- Liang, P., Xu, Y., Zhang, X., Ding, C., Huang, R., Zhang, Z., Lv, J., Xie, X., Chen, Y., Li, Y., et al. (2015). CRISPR/Cas9-mediated gene editing in human triprounuclear zygotes. *Protein Cell* 6, 363–372.
- Lin, Y., Cradick, T.J., Brown, M.T., Deshmukh, H., Ranjan, P., Sarode, N., Wile, B.M., Vertino, P.M., Stewart, F.J., and Bao, G. (2014). CRISPR/Cas9 systems have off-target activity with insertions or deletions between target DNA and guide RNA sequences. *Nucleic Acids Res.* 42, 7473–7485.
- Liu, L., Bailey, S.M., Okuka, M., Muñoz, P., Li, C., Zhou, L., Wu, C., Czerwiec, E., Sandler, L., Seyfang, A., et al. (2007). Telomere lengthening early in development. *Nat. Cell Biol.* 9, 1436–1441.
- Ma, H., Marti-Gutierrez, N., Park, S.W., Wu, J., Lee, Y., Suzuki, K., Koski, A., Ji, D., Hayama, T., Ahmed, R., et al. (2017). Correction of a pathogenic gene mutation in human embryos. *Nature* 548, 413–419.
- Ma, H., Marti-Gutierrez, N., Park, S.-W., Wu, J., Hayama, T., Darby, H., Van Dyken, C., Li, Y., Koski, A., Liang, D., et al. (2018). Ma et al. reply. *Nature* 560, E10–E23.
- Mayrhofer, M., Viklund, B., and Isaksson, A. (2016). Rawcopy: Improved copy number analysis with Affymetrix arrays. *Sci. Rep.* 6, 36158.
- McCoy, R.C., Demko, Z.P., Ryan, A., Banjevic, M., Hill, M., Sigurjonsson, S., Rabinowitz, M., and Petrov, D.A. (2015). Evidence of Selection against Complex Mitotic-Origin Aneuploidy during Preimplantation Development. *PLoS Genet.* 11, e1005601.
- Mrasek, K., Schoder, C., Teichmann, A.C., Behr, K., Franze, B., Wilhelm, K., Blaurock, N., Claussen, U., Liehr, T., and Weise, A. (2010). Global screening and extended nomenclature for 230 aphidicolin-inducible fragile sites, including 61 yet unreported ones. *Int. J. Oncol.* 36, 929–940.
- NAS (2017). National Academies of Sciences, Engineering, and Medicine. Human Genome Editing: Science, Ethics, and Governance (The National Academies Press) <https://doi.org/10.17226/24623>.
- NAS (2020). National Academies of Sciences. Heritable Human Genome Editing (The National Academies Press) <https://doi.org/10.17226/25665>.
- Ottolini, C.S., Newnham, L., Capalbo, A., Natesan, S.A., Joshi, H.A., Cima-domo, D., Griffin, D.K., Sage, K., Summers, M.C., Thornhill, A.R., et al. (2015). Genome-wide maps of recombination and chromosome segregation in human oocytes and embryos show selection for maternal recombination rates. *Nat. Genet.* 47, 727–735.
- Ottolini, C.S., Kitchen, J., Xanthopoulou, L., Gordon, T., Summers, M.C., and Handyside, A.H. (2017). Tripolar mitosis and partitioning of the genome arrests human preimplantation development in vitro. *Sci. Rep.* 7, 9744.
- Sagi, I., De Pinho, J.C., Zuccaro, M.V., Atzmon, C., Golan-Lev, T., Yanuka, O., Prosser, R., Sadowy, A., Perez, G., Cabral, T., et al. (2019). Distinct Imprinting Signatures and Biased Differentiation of Human Androgenetic and Parthenogenetic Embryonic Stem Cells. *Cell Stem Cell* 25, 419–432.e9.
- Sfeir, A., and Symington, L.S. (2015). Microhomology-Mediated End Joining: A Back-up Survival Mechanism or Dedicated Pathway? *Trends Biochem. Sci.* 40, 701–714.
- Sprung, C.N., Reynolds, G.E., Jasin, M., and Murnane, J.P. (1999). Chromosome healing in mouse embryonic stem cells. *Proc. Natl. Acad. Sci. USA* 96, 6781–6786.
- Treff, N.R., Zimmerman, R., Bechor, E., Hsu, J., Rana, B., Jensen, J., Li, J., Samoilenko, A., Mowrey, W., Van Alstine, J., et al. (2019). Validation of concurrent preimplantation genetic testing for polygenic and monogenic disorders, structural rearrangements, and whole and segmental chromosome aneuploidy with a single universal platform. *Eur. J. Med. Genet.* 62, 103647.
- Vanneste, E., Voet, T., Le Caignec, C., Ampe, M., Konings, P., Melotte, C., Debrock, S., Amyere, M., Vikkula, M., Schuit, F., et al. (2009). Chromosome instability is common in human cleavage-stage embryos. *Nat. Med.* 15, 577–583.
- Wright, W.E., Piatyszek, M.A., Rainey, W.E., Byrd, W., and Shay, J.W. (1996). Telomerase activity in human germline and embryonic tissues and cells. *Dev. Genet.* 18, 173–179.
- Wright, D.L., Jones, E.L., Mayer, J.F., Oehninger, S., Gibbons, W.E., and Lanzendorf, S.E. (2001). Characterization of telomerase activity in the human oocyte and preimplantation embryo. *Mol. Hum. Reprod.* 7, 947–955.
- Yamada, M., Johannesson, B., Sagi, I., Burnett, L.C., Kort, D.H., Prosser, R.W., Paull, D., Nestor, M.W., Freeby, M., Greenberg, E., et al. (2014). Human oocytes reprogram adult somatic nuclei of a type 1 diabetic to diploid pluripotent stem cells. *Nature* 510, 533–536.
- Zakarin Safier, L., Gumer, A., Kline, M., Egli, D., and Sauer, M.V. (2018). Compensating human subjects providing oocytes for stem cell research: 9-year experience and outcomes. *J. Assist. Reprod. Genet.* 35, 1219–1225.
- Zuo, E., Huo, X., Yao, X., Hu, X., Sun, Y., Yin, J., He, B., Wang, X., Shi, L., Ping, J., et al. (2017). CRISPR/Cas9-mediated targeted chromosome elimination. *Genome Biol.* 18, 224.

STAR★METHODS

KEY RESOURCES TABLE

REAGENT or RESOURCE	SOURCE	IDENTIFIER
Recombinant DNA		
pCas9_GFP	Addgene	RRID:Addgene_44719
Chemicals, Peptides, and Recombinant Proteins		
EnGen Cas9 NLS	New England Biolabs	M0646T
Quinn's Sperm washing medium	CooperSurgical	ART-1005
Sperm freezing medium	Irvine Scientific	90128
Tris-HCl	Sigma Aldrich	T5941
EDTA	Sigma Aldrich	EDS
Global Total w. HEPES	LifeGlobal	LGTH-050
CytochalasinB	Sigma Aldrich	C2743
Global total	LifeGlobal	H5GT-030
Nocodazole	Sigma Aldrich	M1404-2mg
AmpliTaQ Gold	ThermoFisher	4398886
StemFlex	ThermoFisher	A3349401
Geltrex	Thermo Fisher	A1413302
DMSO	Sigma Aldrich	D2650
Rock inhibitor Y-27632	Selleckchem	S1049
TrypLE Express	LifeTechnologies	12605036
PBS	LifeTechnologies	14190-250
KnockOut Serum Replacement (KO-SR)	LifeTechnologies	10828-028
KO-DMEM	LifeTechnologies	10829-018
Embryonic Stem Cell FBS qualified	Thermo Fisher	16141079
bFGF	Thermo Fisher	PHG0360
Sodium Acetate	Sigma Aldrich	S2889
Ethanol Absolute (200 Proof)	Thermo Fisher	BP2818-500
Glycoblue	Thermo Fisher	AM9515
Critical Commercial Assays		
TaqMan assay	ThermoFisher	C_397916532_10
Affymetrix UK Biobank Axiom Array	ThermoFisher	902502
Deposited Data		
Affymetrix SNP array data from cell lines and human embryos	Gene Expression Omnibus	GEO: GSE1484888
Experimental Models: Cell Lines		
Embryonic stem cell line; genotype: EYS ^{wt} /EYS ^{2265fs}	In house	eyesES1
Embryonic stem cell line; genotype: EYS ^{wt} /EYS ^{indel}	In house	eyesES4
Embryonic stem cell line; genotype: EYS ^{wt} /EYS ^{indel}	In house	eyesES5
Embryonic stem cell line; genotype: EYS ^{wt} /EYS ^{indel}	In house	eyesES6
Embryonic stem cell line; genotype: EYS ^{wt} /EYS ^{2265fs}	In house	eyesES8
Embryonic stem cell line; genotype: EYS ^{wt} /EYS ^{indel}	In house	eyesES9

(Continued on next page)

Continued

REAGENT or RESOURCE	SOURCE	IDENTIFIER
Experimental Models: Organisms/Strains		
Human gametes	Columbia University Fertility Center	n/a
Oligonucleotides		
Oligos for genotyping in Table S7	IDT DNA technologies	Unique DNA sequence provided in Table S7
gRNA for G deletion allele of rs758109813	Synthego	n/a
gBlock for gRNA expression	IDT DNA technologies	sequence provided in Table S7
Biological Samples		
Irradiated MEFs CF-1 MEF 2M IRR	GlobalStem	GSC-6201G
Software and Algorithms		
gSUITE software	Genomic Prediction	n/a
ICE	Synthego	https://ice.synthego.com/#/
Cas9 OFF finder tool	Molecular Genome Engineering Lab, Korea	http://www.rgenome.net/cas-offfinder/
OTHER		
DNA purification kit	ROCHE	11732676001
Male-FactorPak collection kit	Apex Medical Technologies	MFP-130
Piezo micropipette	Origio	Piezo-20-15
10%PVP	Irvine Scientific	90123
Mineral oil	Sigma Aldrich	330779-1L
Holding pipette	Origio	MPH-MED-30
ICSI micropipette	Origio	MIC-SI-30
REPLI-g single cell kit	QIAGEN	150345
TOPO-TA cloning kit	Thermo Fisher	450640
Nucleofection kit	Lonza	VVPH-5012
QuickExtract DNA extraction kit	Lucigen	QE09050
QIAprep Spin Miniprep Kit	QIAGEN	27106

RESOURCE AVAILABILITY

Lead Contact

Further information and requests for resources and reagents should be directed to and will be fulfilled by the Lead Contact, Dieter Egli (de2220@cumc.columbia.edu).

Materials Availability

ESC lines are available upon request.

Data and Code Availability

SNP array data are available at Gene Expression Omnibus (GEO) under accession number GSE148488. Gamete donors provided consent for genetic analysis and public data sharing. This study did not generate code. Genomic Prediction provides preimplantation embryo sample analysis service using gSUITE software.

EXPERIMENTAL MODEL AND SUBJECT DETAILS

Gamete donation

Oocyte donors were recruited from subjects participating in the Columbia Fertility oocyte donor program and were provided the option to donate for research instead of for reproductive purpose. Oocyte donors underwent controlled ovarian stimulation and oocyte retrieval as in routine clinical practice and as previously described ([Zakarin Safier et al., 2018](#)). Oocyte donors also provided a vial of blood (3-5ml) for isolation of genomic DNA using Roche kit. 67 Oocytes from a total of 8 different oocyte donors were used. Age at donation was 27-31. Oocytes were cryopreserved using Cryotech vitrification kit until genotyping of the oocyte donor at mutation site and flanking SNPs was completed and then thawed using the Cryotech warming kit. The sperm donor (age 57 at donation) provided material via Male-FactorPak collection kit (Apex Medical Technologies MFP-130), which was cryopreserved using Quinn's washing

medium from Cooper Surgical and TYB freezing media from Irvine Scientific. Genomic DNA of the sperm donor was isolated from semen using Roche kit. All human embryos were cultured for no more than 1- 6 days, in accordance with internationally accepted standards to limit developmental progression to less than 14 days (ISSCR, 2016). All gamete donors provided signed informed consent. All human subjects research was reviewed and approved by the Columbia University Embryonic Stem Cell Committee and the Institutional Review Board.

Derivation and culture of ESCs

Stem cells were derived after trophectoderm biopsy and plating for the inner cell mass as previously described (Yamada et al., 2014). Briefly, mural trophectoderm was ablated using laser-assisted pulses 400 μ s, 100% intensity (Hamilton Thorne)(Chen et al., 2009). This method spares polar trophectoderm, which usually results in trophectoderm growth which is then ablated with additional pulses. Two stem cell lines with the parental genotypes wt/EYS^{2265fs}, eysES6 and eysES1, were obtained and used for experiments to determine mechanisms of repair after Cas9 mediated cleavage of the eys mutant allele. Derivation was performed on irradiated MEFs (GlobalStem) in KO-DMEM with 25% KO-SR with 10 μ M Rock inhibitor Y-27632, 10ng/mL bFGF and 2% ES grade FBS. Outgrowths were allowed to grow for two weeks until manual passaging and FBS is gradually phased in partial media changes every second or third day. Passaged stem cells a cultured with StemFlex media on Geltrex. Upon reaching 70% confluency, cultures were passaged at a ratio of 1:10, or cryopreserved in a solution of freezing media containing 40% FBS (Company) and 10% DMSO (Sigma Aldrich). Passaging was performed by TrypLE dissociation to small clusters of cells, and plated in media containing Rock inhibitor Y-27632 was added to media and removed within 24-48 h. For later passage cells (> passage 10), Rock inhibitor was omitted. Genotypes are indicated in Table S1. All embryo and ESC research was reviewed and approved by the Columbia University Embryonic Stem Cell Committee and the Institutional Review Board.

METHOD DETAILS

RNP preparation

Guide RNA 5'-GUGUGUCUUCUUCUGUACUGGUUUUAGAGCUAGAAAUAGCAAGUAAAAUAAGGCUAGUCCGUAUCAACUUGAAAAAGUGGCACCGAGUCGGUGCUUUU-3' was obtained from Synthego, with the target RNA underlined. EnGen Cas9 NLS, *S. pyogenes* was obtained from NEB. For ribonucleoprotein (RNP) preparation 3.125 μ L of 20 μ M Cas9 and 0.776 μ L of 100 μ M sgRNA was combined and incubated at room temperature for 10 min, followed by addition of 46 μ L injection buffer consisting of 5mM Tris-HCl, 0.1mM EDTA, pH 7.8.

Oocyte manipulations

All manipulations were performed in an inverted Olympus IX71 microscope using Narishige micromanipulators on a stage heated to 37°C using Global Total w. HEPES. Oocyte enucleation for androgenesis was performed as previously described (Yamada et al., 2014, Sagi et al., 2019). Briefly, oocytes were enucleated in 5 μ g/mL cytochalasinB, the zona pellucida was opened using a zona laser (Hamilton Thorne) set at 100% for 300 μ s. The spindle was visualized using microtubule birefringence and removed using a 20 μ m inner diameter Piezo micropipette (Humagen). Intracytoplasmic sperm injection was identical for both nucleated and enucleated metaphasell oocytes. Cryopreserved sperm was thawed to room temperature for 10 min and transferred to a 15mL conical tube. Quinn's Sperm Washing Medium was added dropwise to a final volume of 6mL. The tube was then centrifuged at 300x g for 15 min. Supernatant was removed and an additional wash was performed. Upon removal of supernatant from second wash, pellet was suspended in wash media and analyzed for viability.

Manipulation dishes consisted of a droplet with 10%PVP, a 10-20 μ L droplet with RNP in injection buffer, and a droplet of Global Total w. HEPES. Sperm was mixed with 10%PVP, and individual motile sperm was immobilized by pressing the sperm tail with the ICSI micropipette, picked up and ejected in the Cas9 RNP droplet and picked up again for injection. ICSI without immersion in the Cas9 RNP droplet was also performed. After all manipulations, cells were cultures in Global total in an incubator at 37°C and 5% CO₂. Pronucleus formation was confirmed on day 1 after ICSI. 2-cell injections were performed at least 3 h after cleavage, between 30-35 h post ICSI. Earlier injection resulted in lysis. The tip of an injection needle was nicked and small amounts of the Cas9RNP was injected manually using a Narishige micromanipulator.

Genome amplification and Genotyping

Zygotes were collected at 20 h post ICSI, and single blastomeres were collected on day3 to day4. Trophectoderm biopsies were obtained on day6 of development using 300ms laser pulses to separate trophectoderm from the inner cell mass. Single zygote nuclei were extracted from zygotes in the presence of 10 μ g/mL CytochalasinB and 1 μ g/mL nocodazole at 20 h post ICSI. All samples were placed in single tubes with 2 μ L PBS. Amplification was performed using REPLI-g single cell kit (QIAGEN Cat #150345) according to manufacturer's instructions. Illustra GenomePhi V2 DNA amplification kit (GE Healthcare 95042-266) was also used. REPLI-g was used in most experiments as it resulted in more genomic DNA product. Genotyping was performed using primers for amplification and sequencing as listed in Table S7. PCR was performed using AmpliTaq Gold. PCR products were loaded on gel for visual inspection of product size. PCR products were submitted to Genewiz for Sanger sequencing. If two bands were detected, both were sequenced separately after TOPO cloning. PCR artifacts were distinguished from genuine products by Sanger sequencing and blast

search analysis (NCBI blastn) whether the sequence mapped to the EYS locus. TOPO-TA cloning was done also for heterozygous edits and 5-10 bacterial colonies were used for Miniprep preparation and sequenced to identify the two edits individually (e.g., Figure 1F).

For on-target NGS shown in Figures 1C, 1D, and 4C, primers were designed to amplify rs66502009 and the EYS^{2265fs} mutation rs758109813 (as shown in Figure 1A and Table S7). PCR products were purified via sodium acetate precipitation and submitted for AmpliconEZ sequencing at Genewiz. Results were provided in the format of raw reads and fastq files and an analysis of read frequency was conducted. Each sample yielded > 50,000 reads. Sequences with a read count that exceeded 0.2% of the total reads (> 100 reads) were considered significant. Those that had less than 100 reads were considered insignificant due to the possibility that these were due to sequencing errors or mutations introduced during DNA amplification. Base changes were analyzed at the region of Cas9 cutting, and paternal and maternal alleles were called based on rs66502009, and rs758109813 (EYS^{2265fs}).

Cas9 off-target analysis was performed by identifying potential off-target sites using Cas-OFF finder online tool (<http://www.genome.net/cas-offfinder/>), selecting SpCas9 of *Streptococcus pyogenes*. 32 potential off-target sites were predicted across 14 chromosomes. Those with 3 or fewer mismatches were selected for analysis. PCR primers for off-target analysis are indicated in Table S7.

EYS mutation allelic discrimination qPCR

A TaqMan assay (C_397916532_10) was used to obtain allelic discrimination results for the EYS mutation (rs758109813; NG_023443.2:g.1713111del) using a QuantStudio 3 instrument and following the manufacturer's recommendations (ThermoFisher). See Table S5 for results.

Genome-wide SNP array

Embryo biopsies were amplified at Columbia University using either REPLI-g or GenomePhi as described above, or at Genomic Prediction Clinical Laboratory using ePGT amplification (Treff et al., 2019). Amplified DNA was processed according to the manufacturer's recommendations for Axiom GeneTitan UKBB SNP arrays (ThermoFisher). Copy number and genotyping analysis was performed using gSUITE software (Genomic Prediction). Parental origin of copy number changes was determined by genotype comparison of embryonic and parental SNPs. For copy number analysis, raw intensities from Affymetrix Axiom array are first processed according to the method described (Mayrhofer et al., 2016). After normalizing with a panel of normal males, the copy number is then calculated for each probet. Normalized intensity is displayed. Mapping of endogenous fragile sites was done through visual evaluation of loss of heterozygosity. Break points were mapped to chromosomal bands by visual analysis of SNP array chromosome plots including analysis of both copy number signal and heterozygosity calls. The accuracy of mapping is between 100-500kb. Evaluation whether a segmental error involved a common fragile site was performed by comparison of break sites to the location of common fragile sites according to (Mrasek et al., 2010).

DSB repair in EYS^{wt}/EYS^{2265fs} ESCs

For CRISPR-Cas9 gene editing, cultures of embryonic stem cell lines eysES1 and eysES6, both of which have the EYS^{wt}/EYS^{2265fs} genotype and are heterozygous at rs66502009 were dissociated to single cells, and cells were nucleofected with pCas9_GFP (Addgene #44719) (Ding et al., 2013), a gBlock (IDT) expression vector, using the Lonza Kit and Amaxa Nucleofector. 1 million cells at 50% confluency at time of use were nucleofected per reaction using program A-023. GFP positive cells were sorted using BD SORP FACSARIA cell sorters 48 h post nucleofection at the Columbia Stem Cell Initiative Flow Cytometry Core.

For NGS analysis as shown in Figures 1C and 1D, 2000-5,000 sorted cells were harvested for genome amplification using identical methods as used for embryo blastomeres. Whole genome amplification was performed using REPLI-g (QIAGEN). PCR was then performed using primers flanking EYS^{2265fs} and rs66502009 and products were analyzed for gene editing using AmpliconEZ service of Genewiz. Read frequency analysis was used to quantify molecularly distinct edits. Paternal and maternal alleles were distinguished based on EYS^{2265fs} and rs66502009.

For clonal analysis shown in Figure 1E, two independent experiments with eysES1 and eysES6 were performed. Single Cas9-GFP positive sorted cells were plated in individual wells of 96-well plates onto Geltrex with StemFlex media with Rock inhibitor Y-27632. After 5-12 days, colonies were picked and harvested for DNA isolation and analysis. DNA collection from cultured cells was performed using QuickExtract. PCR and sequencing was performed using primers flanking the gRNA at EYS^{2265fs} as well as rs66502009. The paternal and maternal alleles were identified using rs66502009 and EYS^{2265fs}, and Cas9-induced modifications were called through visual analysis and using ICE (<https://ice.synthego.com/#/>). Sanger profiles from all edited colonies contained at most two molecularly different alleles, and equal signal intensity from the edited paternal allele and from the non-edited maternal allele, confirming that they were individual events originating from single cells.

QUANTIFICATION AND STATISTICAL ANALYSIS

Statistical analysis of different genotypes was performed using Fisher's exact test as indicated in the figure legends.

Supplemental Figures

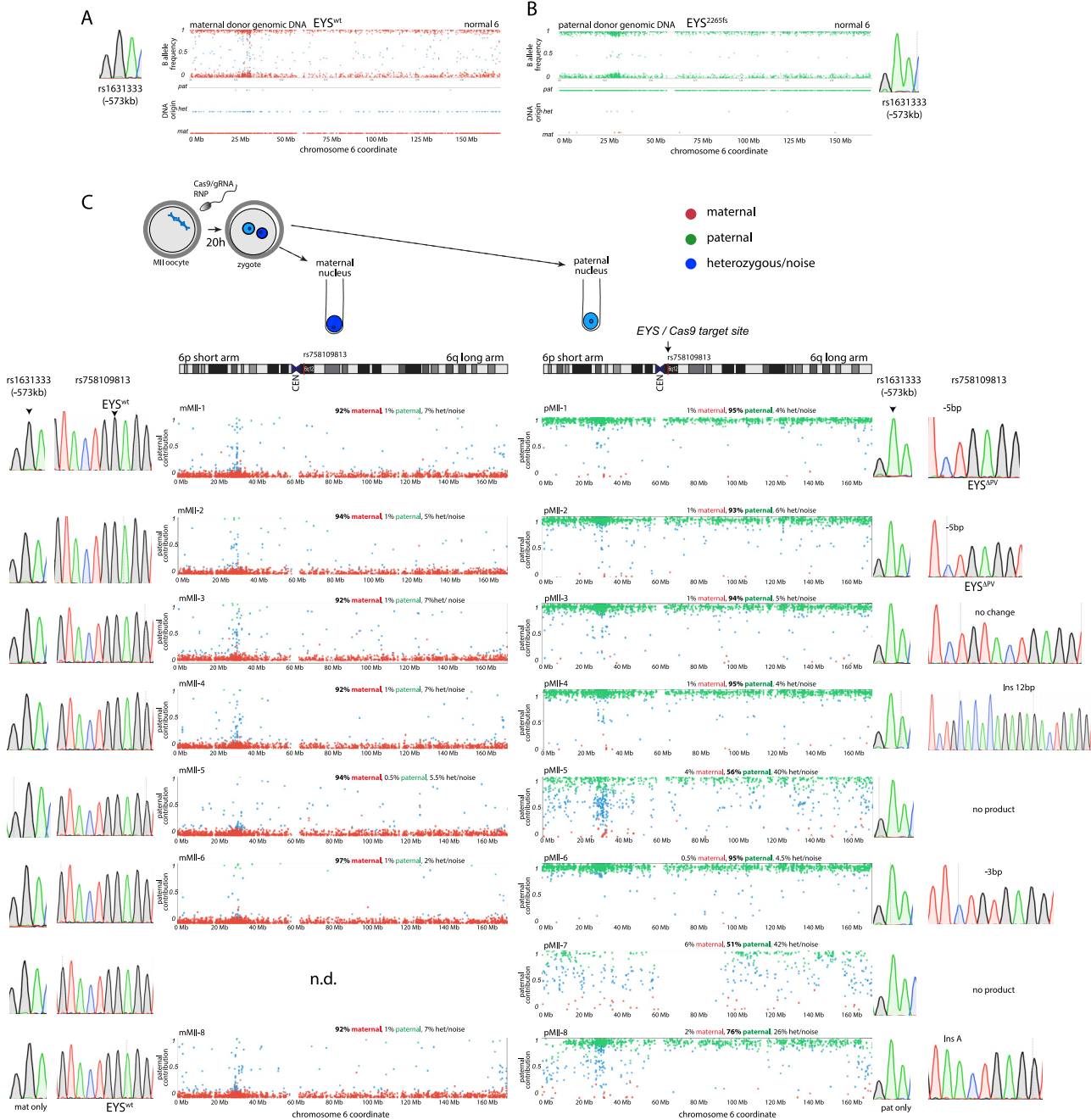


Figure S1. Parent-of-Origin Analysis of Paternal and Maternal Nuclei using SNP Arrays, Related to Figure 2

(A and B) SNP array analysis of paternal and maternal genomic DNA. Increased signal intensity is seen in the HLA region of chromosome 6, which shows increased background signal. Paternal and maternal alleles are displayed as B allele frequency with DNA origin inferred below. Information on the molecular identity of A and B alleles is available with the GEO submission GSE148488 under file name GPL28377 Affymetrix Axiom UK Biobank. In (A) is an analysis of amplified gDNA from cumulus cells of egg donor A as a control for a maternal-only chromosome 6 array profile, and in (B) is an analysis of paternal genomic DNA as a control for a paternal-only SNP array profile.

(legend continued on next page)

(C) Analysis of paternal and maternal single nuclei isolated from eight 2PN zygotes at the 1-cell stage, 20 h post fertilization and Cas9 RNP injection. On top, shown is the chromosomal location of the Cas9 target site at the EYS locus. The SNP array plots show paternal allele frequency. Only SNPs in which the maternal genotype was homozygous for one allele (red) and the paternal genotype was homozygous for the other allele (green) were used for analysis. Quantification of allelic frequencies is shown above the plots and in Table S4. up = chr6:1-64.7Mb, and down = chr6:64.7Mb-telomere. n.d., not determined. Related to [Figure 2](#). Sanger profiles from MII-8 and MII-5, and SNP array results from MII-5 are also shown in [Figure 2](#). For SNP array analysis of other autosomes see [Table S3](#).

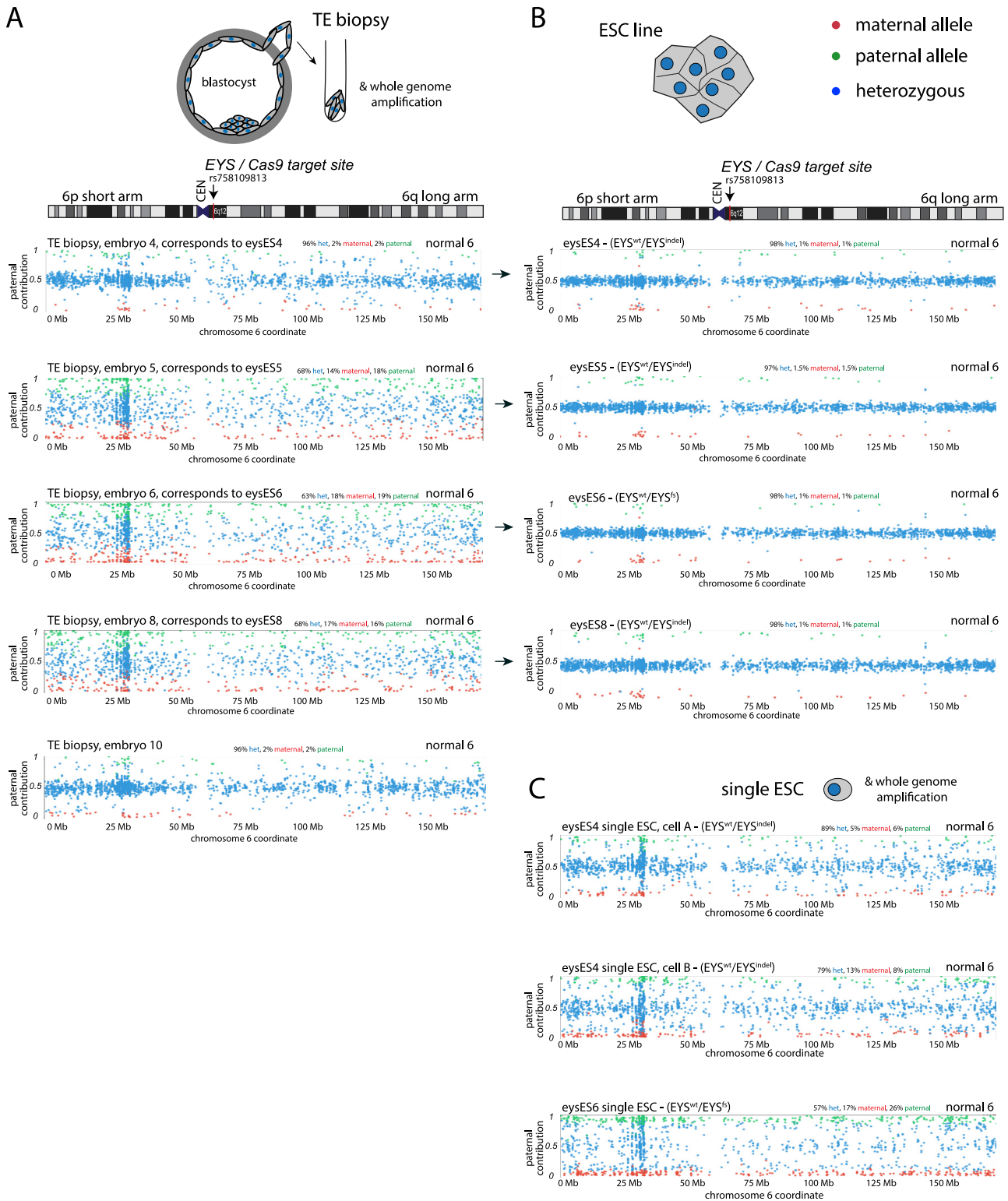


Figure S2. Heterozygosity in Blastocysts and Derived Stem Cell Lines on Chromosome 6 after Cas9 RNP Injection at the MII Stage, Related to Figures 2, 3, 4, and 5

SNP array analysis of blastocysts and stem cell lines. For each graphic, the developmental stage of the biopsy is indicated by a schematic at the top. The chromosomal location of the Cas9 target site at the *EYS* locus (arrow) is shown above the plots.

(legend continued on next page)

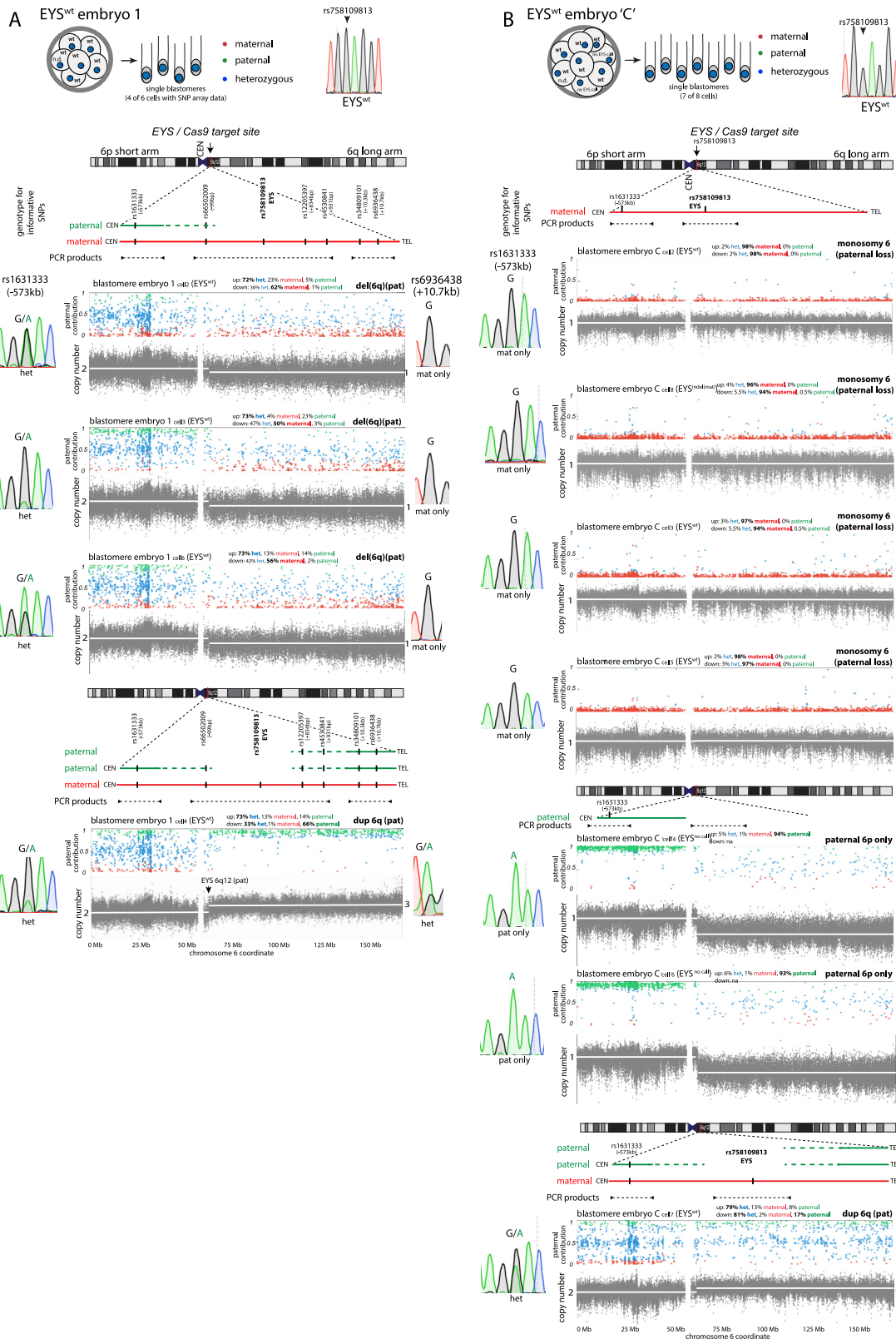
SNP array plots show paternal allele frequency. Only SNPs in which the maternal genotype was homozygous for one allele (red) and the paternal genotype was homozygous for the other allele (green) were used for analysis. Quantification of allelic frequencies is shown above the plots. up = chr6:1-64.7Mb, and down = chr6:64.7Mb-telomere.

(A) Blastocyst biopsies. Each plot is a different blastocyst, four of which gave rise to a pluripotent stem cell line (horizontal arrows). The on-target genotype of the TE biopsies could not be determined.

(B) Chromosome 6 SNP array analysis of embryonic stem cell lines as a positive control for detection of heterozygosity along chromosome 6.

(C) The same stem cell lines are analyzed by SNP array after whole genome amplification from single cells. Heterozygous alleles detected at equal ratios are shown in blue, while unequal ratios of maternal and paternal alleles present as either red or green. This is the consequence of allelic bias during whole genome amplification from single cells using REPLI-G.

For SNP array analysis of other autosomes see [Table S3](#), for quantification of alleles see [Table S4](#).



(legend on next page)

Figure S3. Chromosomal Rearrangements at the EYS Locus in Blastomeres after Cas9 RNP Injection at the MII Stage, Related to Figure 3

SNP array analysis of embryos without the paternal *EYS*^{rs2265fs} allele. For each panel, the biopsied embryo is indicated by a schematic at the top, and the number of cells successfully isolated and analyzed by SNP array is indicated with the number of tubes. The plots show paternal allele frequency (top plot), and copy number (gray plot). Only SNPs in which the maternal genotype was homozygous for one allele (red) and the paternal genotype was homozygous for the other allele (green) were included. Blue indicates a heterozygous (normal) embryo genotype. Quantification of allelic frequencies is shown above the plots. up = chr6:1-64.7Mb, and down = chr6:64.7Mb-telomere. (A) and (B) are two different embryos. Sanger sequencing calls of rs1631333 were validated with selected on-target deep sequencing (Table S2).

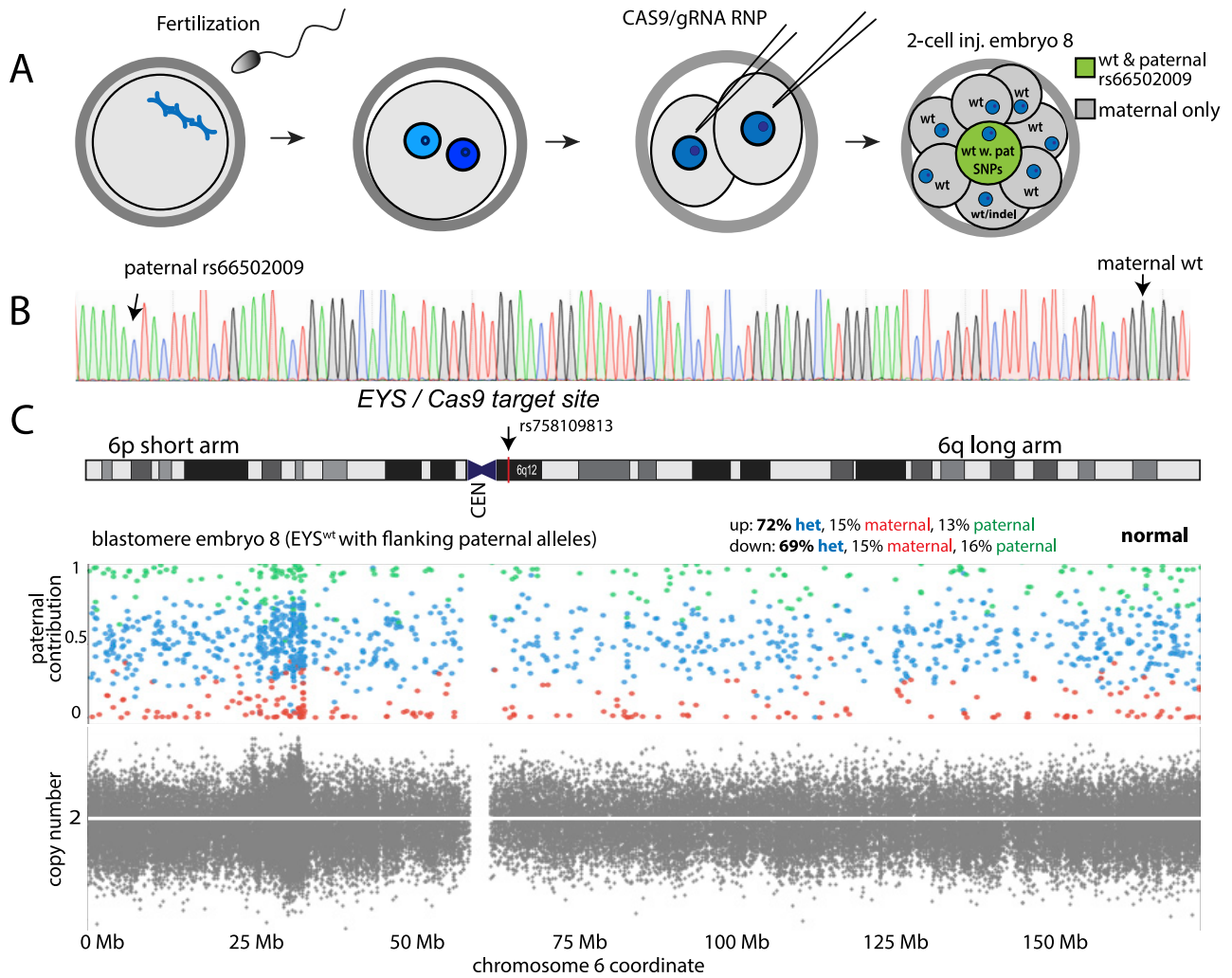


Figure S5. Possible Interhomolog Repair Event after Injection at the Two-Cell Stage, Related to Figure 4

(A) Schematic of the experiment. Injection of Cas9/RNP at the 2-cell stage, one cell cycle after fertilization, and when paternal and maternal genomes are contained within the same nucleus.

(B) Novel linkage of maternal EYS^{wt} SNP and paternal rs66502009 shown by Sanger sequencing.

(C) The SNP array plots shows paternal allele frequency (top plot) and copy number analysis (gray) for chromosome 6. Only SNPs in which the maternal genotype was homozygous for one allele (red) and the paternal genotype was homozygous for the other allele (green) were included. Blue indicates a heterozygous (normal) embryo genotype. Quantification of allelic frequencies is shown above the plots. up = chr6:1-64.7Mb, and down = chr6:64.7Mb-telomere. The cell is heterozygous throughout chromosome 6 and carries an EYS^{wt} only genotypes at the mutation site with paternal flanking SNPs. CEN = centromere. For SNP array analysis of other autosomes see [Table S3](#).

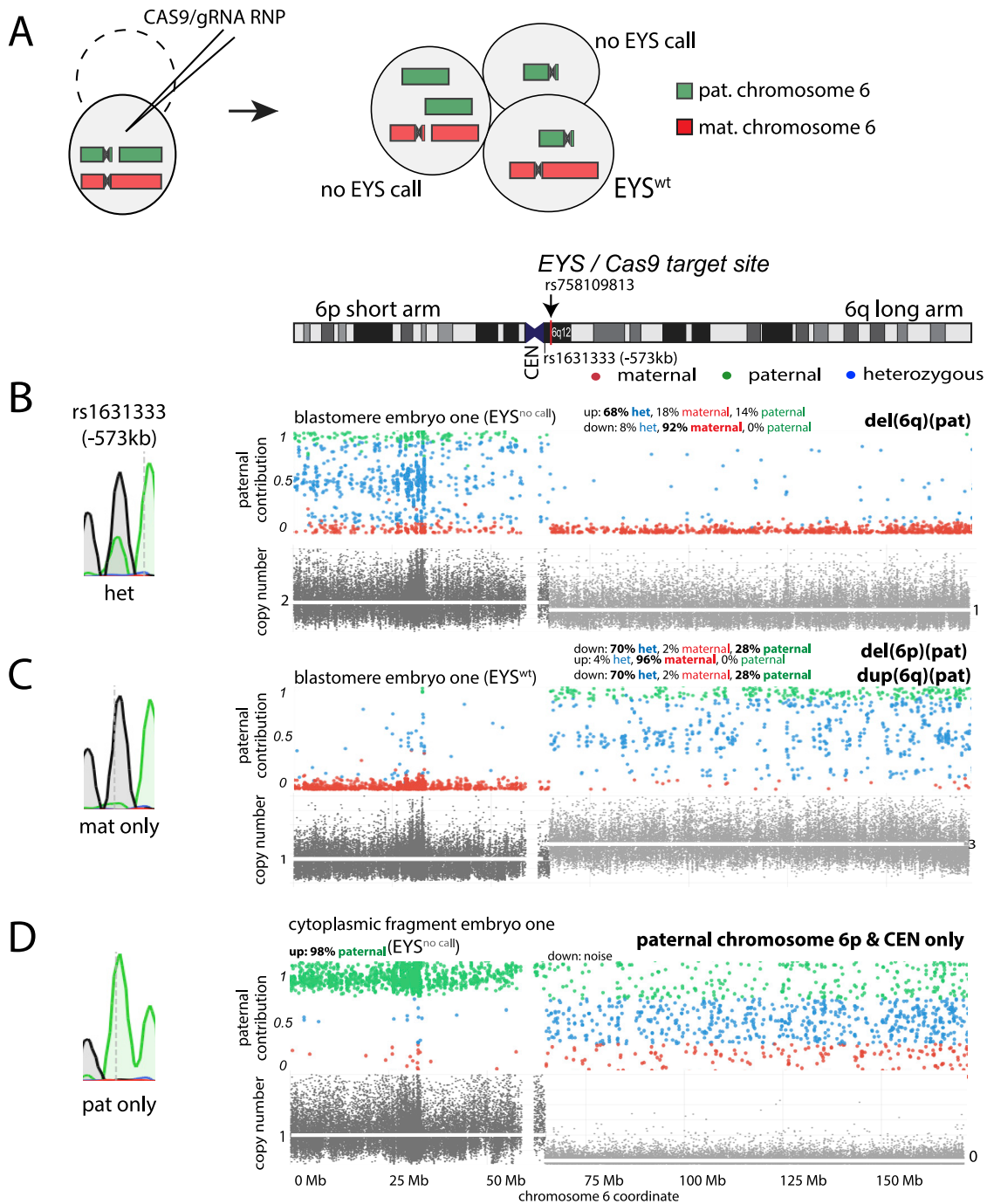
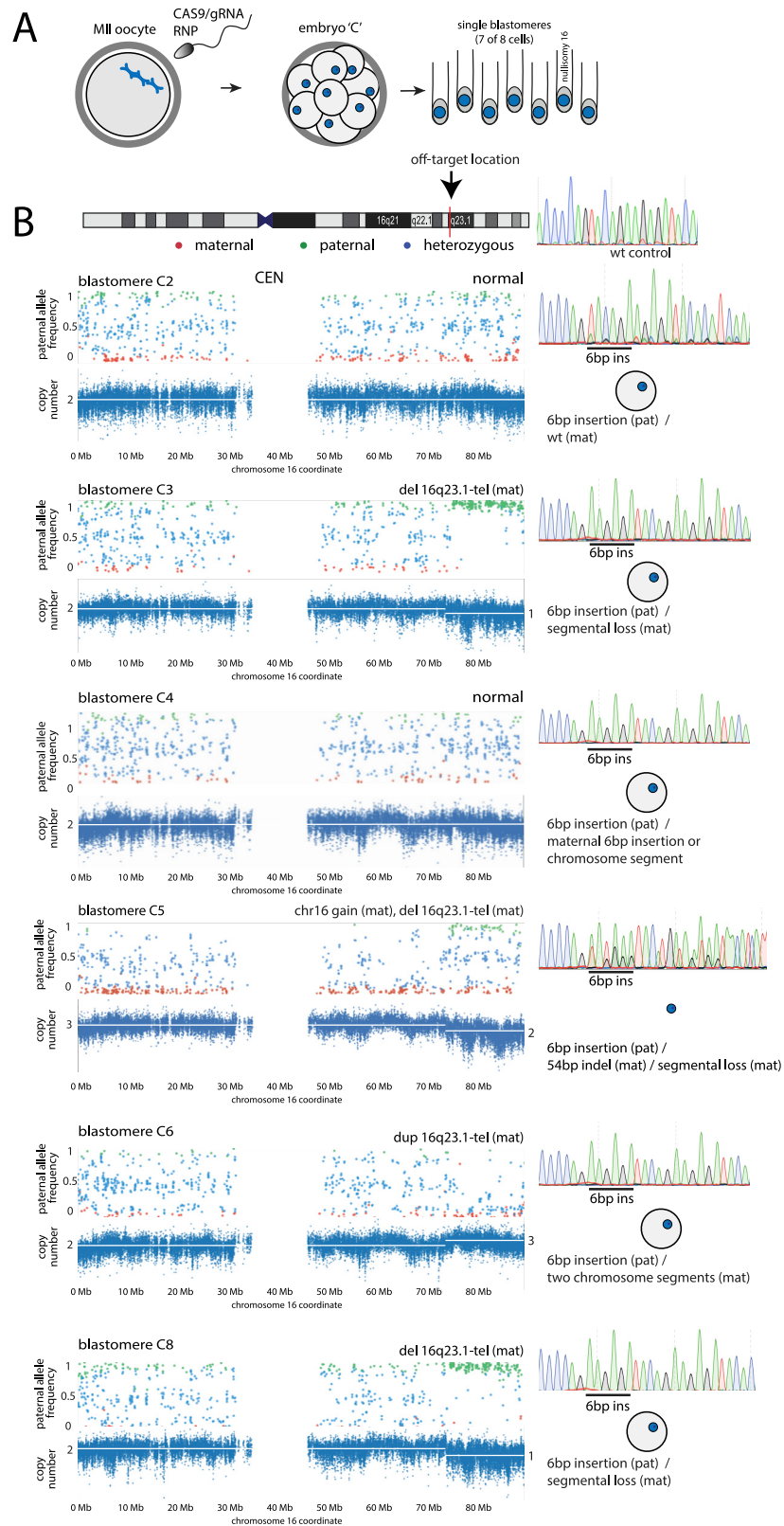


Figure S6. Chromosome Loss after Cas9 RNP Injection into Two-Cell Stage Embryos, Related to Figure 4

(A) Schematic of the cell division products observed after a single cell cycle post Cas9 RNP injection. Three cells/fragments were successfully analyzed. Dotted circle indicates another cell of the same 2-cell embryo without a result.

(B–D). Sanger sequencing of rs1631333 and corresponding SNP arrays for 2 different cells (B) and (C) and one cytoplasmic fragment (D). Shown is the chromosomal location of the Cas9 target site at the *EYS* locus and the SNP rs1631333 informative of parental origin. The plots show paternal allele frequency and copy number analysis (gray). Only SNPs in which the maternal genotype was homozygous for one allele (red) and the paternal genotype was homozygous for the other allele (green) were used for analysis. Blue indicates a heterozygous (normal) embryo genotype. Quantification of allelic frequencies is shown above the plots. up = chr6:1-64.7Mb, and down = chr6:64.7Mb-telomere. The area centromeric of the *EYS* gene and 6p are shaded in a dark gray, 6q telomeric of *EYS* in a lighter gray. (B) Cell with a loss of chromosome 6q (C) cell with a loss of chromosome 6p and a gain of chromosome 6q, and (D) 'cell' with only chromosome 6p without any other genomic DNA. The signal on the q arm is background/noise. Note that the cleavage products add up to 2 copies for each 6p and 6q arm. CEN = centromere. (B) and (C) are also related to [Figure 5](#).



(legend on next page)

Figure S7. Segmental Chromosome Loss Due to Cas9 Off-Target Activity on Chromosome 16, Related to Figures 5 and S3B

(A) Schematic of the experiment. Injection of Cas9 RNP at the MII stage and collection for analysis at the cleavage stage. One cell gave no result because of nullisomy for chromosome 16.

(B) SNP array analysis of embryo C. The location of the off-target site on chromosome 16 is shown (arrow). Only SNPs in which the maternal genotype was homozygous for one allele (red) and the paternal genotype was homozygous for the other allele (green) were used for analysis. Plot 2 (blue) indicates copy number. Corresponding Sanger profiles are provided on the right. Note uniform insertion of 6bp in one allele in all blastomeres (underlined), and mosaicism for the other allele, including segmental chromosomal aneuploidies, as well as a 54bp long indel in one cell. The insertion of 6bp is a duplication, which may be caused by microhomology-mediated break-induced replication (Hastings et al., 2009), though this remains to be determined. Mosaicism of this embryo shows that off-target activity of Cas9 continues after the 1-cell stage. CEN = centromere.